PERGAMON

Vision Research 41 (2001) 2845–2872

Vision Research

www.elsevier.com/locate/visres

Neural model for processing the influence of visual orientation on visually perceived eye level (VPEL)

Leonard Matin *, Wenxun Li *

Clarence H. Graham Memorial Laboratory of Visual Science, Department of Psychology, Columbia University, New York, NY 10027, USA

Received 12 April 1999; received in revised form 24 November 2000

Abstract

An individual line or a combination of lines viewed in darkness has a large influence on the elevation to which an observer sets a target so that it is perceived to lie at eye level (VPEL). These influences are systematically related to the orientation of pitched-from-vertical lines on pitched plane(s) and to the lengths of the lines, as well as to the orientations of lines of 'equivalent pitch' that lie on frontoparallel planes. A three-stage model processes the visual influence: The first stage parallel processes the orientations of the lines utilizing 2 classes of orientation-sensitive neural units in each hemisphere, with the two classes sensitive to opposing ranges of orientations; the signal delivered by each class is of opposite sign in the two hemispheres. The second stage generates the total visual influence from the parallel combination of inputs delivered by the 4 groups of the first stage, and a third stage combines the total visual influence from the second stage with signals from the body-referenced mechanism that contains information about the position and orientation of the eyes, head, and body. The circuit equation describing the combined influence of n separate inputs from stage 1 on the output of the stage 2 integrating neuron is derived for $\boldsymbol{n}$ stimulus lines which possess any combination of orientations and lengths; Each of the $\boldsymbol{n}$ lines is assumed to stimulate one of the groups of orientation-sensitive units in visual cortex (stage 1) whose signals converge on to a dendrite of the integrating neuron (stage 2), and to produce changes in postsynaptic membrane conductance (g_i) and potential (V_i) there. The net current from the n dendrites results in a voltage change (V_A) at the initial segment of the axon of the integrating neuron. Nerve impulse frequency proportional to this voltage change signals the total visual influence on perceived elevation of the visual field. The circuit equation corresponding to the total visual influence for $\boldsymbol{n}$ equal length inducing lines is $V_A = \Sigma V_i/[n + (g_A/g_S)]$, where the potential change due to line i, V_i, is proportional to line orientation, g_A is the conductance at the axon's summing point, and $g_S = g_i$ for each i for the equal length case; the net conductance change due to a line is proportional to the line's length. The circuit equation is interpreted as a basis for quantitative predictions from the model that can be compared to psychophysical measurements of the elevation of VPEL. The interpretation provides the predicted relation for the visual influence on VPEL, **V**, by $\boldsymbol{n}$ inducing lines each with length $\boldsymbol{l}$: thus, $\mathbf{V} = \boldsymbol{a} + [k_i\Sigma\theta_i/\boldsymbol{n} + (k_2/\boldsymbol{l})]$, where θ_i is the orientation of line i, $\boldsymbol{a}$ is the effect of the body-referenced mechanism, and k_1 and k_2 are constants. The model's output is fitted to the results of five sets of experiments in which the elevation of VPEL measured with a small target in the median plane is systematically influenced by distantly located 1-line or 2-line inducing stimuli varying in orientation and length and viewed in otherwise total darkness with gaze restricted to the median plane; each line is located at either 25° eccentricity to the left or right of the median plane. The model predicts the negatively accelerated growth of VPEL with line length for each orientation and the change of slope constant of the linear combination rule among lines from 1.00 (linear summation; short lines) to 0.61 (near-averaging; long lines). Fits to the data are obtained over a range of orientations from $-30°$ to $+30°$ of pitch for 1-line visual fields from lengths of 3° to 64°, for parallel 2-line visual fields over the same range of lengths and orientations, for short and long 2-line combinations in which each of the two members may have any orientation (parallel or nonparallel pairs), and for the well-illuminated and fully structured pitchroom. In addition, similar experiments with 2-line stimuli of equivalent pitch in the frontoparallel plane were also fitted to the model. The model accounts for more than 98% of the variance of the results in each case. © 2001 Elsevier Science Ltd. All rights reserved.

Keywords: Visually perceived eye level; VPEL; Spatial summation; Space perception; Computational model; Elevation; Visual pitch; Spatial orientation

---

* Corresponding authors.
E-mail addresses: matin@columbia.edu (L. Matin), wl18@columbia.edu (W. Li).

0042-6989/01/$ - see front matter © 2001 Elsevier Science Ltd. All rights reserved.
PII: S0042-6989(01)00150-X

1. Introduction

We normally assume that the spatial locations and orientations at which objects appear are veridical and that if we reach for them we will touch them. Although we carry these same assumptions along with us from place to place we are not generally aware of how highly dependent the veridicality of our perceptions and the successes of our sensorimotor behavior are on the existence of the common aspects of visual stimulation in the many different spatial environments in which we normally spend our lives. Departures from these normal conditions can produce large errors in both our perceptions and our sensorimotor behavior. Some of the important common properties of the visual field underlying the normal stability of our perceptions of space have been studied in laboratories of perception by disturbing these common aspects of stimulation and measuring the resulting illusions psychophysically. For example, the well-known experiments on the tilted-room/tilted-rod (or rod-and-frame) illusion (Asch & Witkin, 1948; Witkin & Asch, 1948; Witkin, 1949) are based on the fact that the main lines of organization of visual fields in both natural and carpentered environments normally run along the horizontal and vertical specified relative to the direction of gravity, and others are based on the fact that the main lines in our visual environment are generally stationary (Brandt, Dichgans, & Koenig, 1973; Held, Dichgans, & Bauer, 1975).[1] Large-field illusions also result from abnormal magnitudes and/or directions of the gravitoinertial force (Graybiel, 1952; Cohen, 1973, 1981; Lackner, 1978; Lackner & Graybiel, 1978). In these latter cases, although the peculiar aspect of the stimulus is the change in the gravitoinertial force, the illusory consequences for the visual perception of space are generally the most striking.

Our laboratory as well as those of others has been working toward understanding a constellation of peculiar spatial errors in perception and sensorimotor behavior that result from pitching the visual field; we have referred to this constellation as the spatial disorientation syndrome produced by visual pitch (SDSPVP) (Matin & Fox, 1986, 1989, 1990; Stoper & Cohen, 1989; Stoper & Bautista, 1991; Li & Matin, 1990c, 1991a,b, 1992, 1993, 1995a,b, 1996, 1997b, 1998, 1999, 2001a,b; Matin & Li, 1991, 1992a,b, 1994a,b,c, 1995a,b, 1997a,b,c, 1998, 1999a, 2000, 2001; Dallal, Li, & Matin, 1993; DiZio, Li, Lackner, & Matin, 1993, 1997; Nemire & Cohen, 1993; Servos, Matin, & Goodale, 1993, 1995; Raphel & Barraud, 1994; Robison, Li, & Matin, 1995; Chelette, Li, Esken, & Matin, 1995; Cohen, Ebenholtz, & Linder, 1995; Post & Welch, 1996; Welch & Post, 1996; Raphel, Barraud, Koessler, & Cian, 1996; Poquin, Ohlmann, & Barraud, 1998; Welch, Post, Lum, Kang, Napoli, & Cohen, 1998; Li, Hudson, & Matin, 2000; Post, Welch, & Clark, 2000; Matin, Li, Hudson, & Hirsch, 2001; Li, Dallal, & Matin, 2001). This constellation includes large misperceptions of the elevation, orientation, size, and height of objects viewed against the background of the pitched visual field, and significant errors in manual localization as well as whole-body disturbances. We have been able to define, isolate, and quantify the basic aspect of the proximal visual stimulus that underlies SDSPVP, and to demonstrate its identity with the basic aspect of the visual influence of roll-tilt on the perception of the vertical in the rod-and-frame illusion (Matin & Li, 1994c, 1995a, 1999b, 2001).

The effects of viewing a stationary pitched visual field in generating SDSPVP were first examined in the pitchroom in which the entire complexly-structured and well-illuminated visual environment of an observer who is seated on the stationary level ground of the building is subjected to pitch—that is, to rotation around a horizontal axis through a plane parallel to a the observer's frontal plane.[2] The pitched visual field consists of a

---

[1] Several of these departures from normality are nicely exemplified in a number of natural and seminatural whole-field illusions such as those at the well-known Mystery Spot at Santa Cruz, California where distortions of some visual features of the environment lead to a number of interesting perceptual errors, including plumb lines appearing askance as if being held out by unseen forces, water running uphill, and errors in the perceived size of people. The failure on the part of visitors to the Mystery Spot to recognize the peculiarities of the features of the visual environment that gives rise to the different illusions, or even to recognize that it is the *visual* environment that is the basis for the peculiar effects, has provided the basis for the owners' ability to market it as a 'gravitational warp' or 'magnetic disturbance' that has baffled scientists. The dramatic quality of these phenomena has inspired similar peculiar beliefs in others as well. Large-field illusions are sometimes shown with less hype in public exhibits, although sometimes with either speculative or inaccurate explanations along more traditional lines than those noted for the Mystery Spot above, and others are present in many other normal situations where the basis is more readily discernible to the observer, such as when sitting in a stationary train but feeling motion in the direction opposite to the direction of motion of another train that suddenly appears in view on the neighboring track.

[2] Most, if not all of the interesting phenomena that can be experienced at the Santa Cruz Mystery Spot are also experienced in the pitchroom, including plumb lines and people looking askance, people made to look smaller or larger, manual mislocalization, and water and balls running uphill, and some can be produced in the pitchroom that are not available at the Mystery Spot. The pitchroom allows us to vary the magnitudes of the effects systematically and generate effects that are considerably larger than those at the Mystery Spot. The original motivation for the construction of the pitchroom was the need for a research device to examine quantitatively predictions based on the results of experiments that we had carried out on observers partially paralyzed by curare, (Matin et al., 1982; Matin, Stevens, & Picoult, 1983). In the curare experiments large systematic spatial mislocalizations of a single light in darkness were psychophysically measured on observers with paretic extraocular muscles; some of these mislocalizations were essentially eliminated by the presence of normal room illumination. The predictions from those results that visual pitch viewed by normal observers would generate systematic effects on the elevation of VPEL were amply confirmed in the pitchroom.

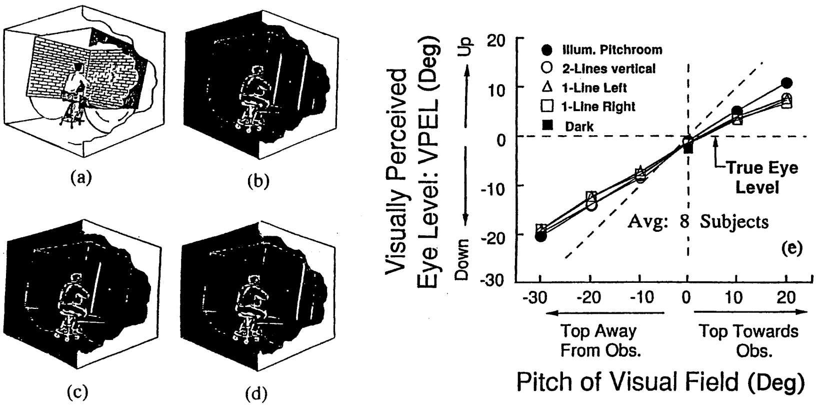

Fig. 1. The pitchroom in its normally illuminated condition with the complexly structured visual field visible to the observer is shown in (a); in (b), (c), and (d) the pitchroom is shown in its totally dark condition with only the 2-line or one of the 1-line stimuli visible along with the laser target employed for measuring VPEL. The pitchroom is shown in topbackward orientation within an erect exterior room in each of the panels. Pitch was varied by rotating the pitchroom on rockers resting on the floor of the exterior room in the directions of the arrows on the righthand rocker in (a). During experiments for the conditions with the fully illuminated pitchroom, a black cloth was attached to the front of the chinrest, hung around the observer's shoulders, and attached to the bottom of the front surface of the pitchroom so that the floor of the exterior room was not visible. Each of the lines in (b), (c) and (d) was vertical when the pitchroom was erect. The arrows above and below the projection of the laser target in (a) indicate the directions in which the laser-generated target was adjusted during psychophysical measurement. (e) Average values of VPEL for eight monocularly-viewing subjects at each of six pitches in the illuminated pitchroom, with the 2-line pitched-from-vertical stimulus, with each of the two pitched-from-vertical 1-line stimuli, and in total darkness. Viewing distance, measured along the normal line of visual direction from the eye was 1 m to the front surface under all conditions.

rectangular room-sans-floor with a front wall facing the observer, two side walls, and a ceiling (Matin & Fox, 1986, 1989; Fig. 1a). Our subsequent investigations have continued to employ the pitchroom, but, since at least some of the major segments of SDSPVP are almost as strong with the entire visual field consisting of as little as a single line in otherwise total darkness, much of the subsequent work has been carried out with individual lines and with pairs and trios of lines, both in the totally darkened pitchroom and out of it, as well as in human centrifuges in which we have been able to modify the gravitational background for the visual stimulus (DiZio et al., 1993, 1997; Chelette et al., 1995). This work has been done with normal observers, as well as with a well-studied visual agnosic (Servos et al., 1995). The present article carries this work further and presents a neural model that describes the mechanism responsible for processing the significant aspects of the visual stimulus that generates one of the main characteristics of SDSPVP—the large systematic deviations in the physical elevation corresponding to eye level.

The psychophysical measurements that will be modeled in the present article are settings by observers of a small, dim, circular visual target to appear at eye level (setting of the elevation of the target to visual perceived eye level, VPEL) under various conditions of structure and pitch and/or roll-tilt of the visual field with a normal 1g gravitational background. In total darkness with no visible lines or other visible stimuli present, individual observers typically set a target to VPEL within a few degrees of true eye level (TEL) with variability (measured by the average standard deviation across pitches and subjects) equal to about 1°. The fundamental observation of the influence of visual pitch on the elevation of VPEL is as follows: With the field of view of the erect observer filled by the pitchroom and the observer facing the pitched surface, a target that remains at the TEL of the observer appears to lie below TEL with the visual field pitched topforward, and to lie above TEL with the visual field pitched topbackward. In correspondence with this, the VPEL setting lies above TEL with the visual field pitched topforward and below TEL with the visual field pitched topbackward; the magnitude of the deviation of VPEL from TEL increases with the pitch magnitude. Over the 75° range of pitch that has been examined the elevation of the VPEL setting changes linearly with a slope of the VPEL-versus-pitch function that averages somewhat more than 0.6 with errors as large as −25° (topbackward) and +11° (topforward) at the extreme ends of the range. Large but stable differences in slope have been measured across individual observers; slopes of different individuals have ranged from 0.17 to 0.86. Although the setting of the elevation of VPEL provides measurements of only a single point within the dimension of perceived elevation, a shift of the elevation of VPEL upward or downward is part of an essentially undistorted shift of the relation between the entire dimension of perceived elevation and physical elevation (Robison et al., 1995; Li & Matin, 1999). Although this shift can be treated as a translation of the perceived vertical dimension relative to the physical vertical di-

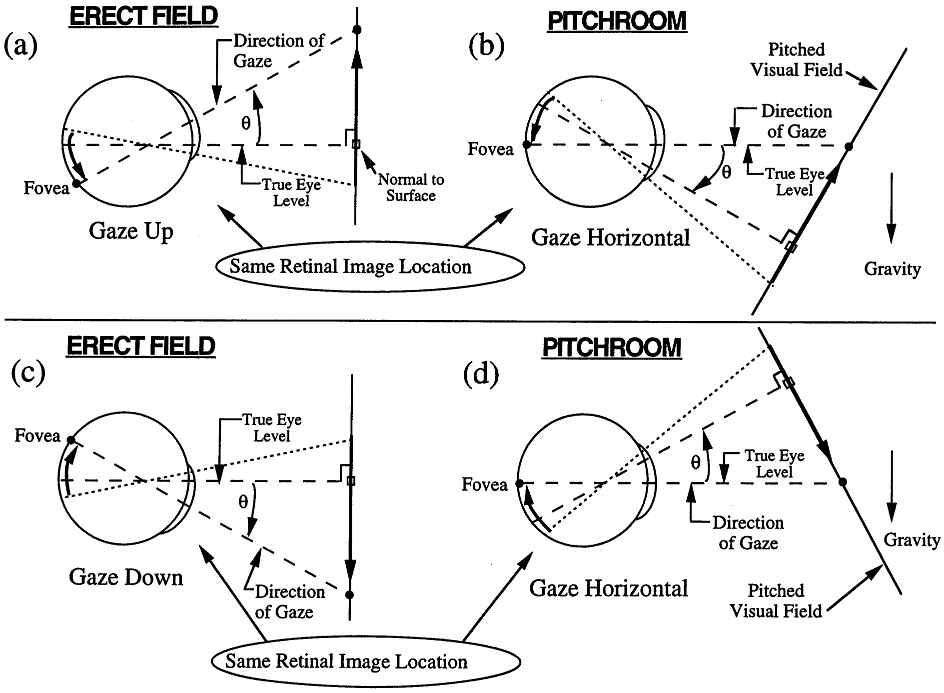

Fig. 2. (a) and (b) Setting the pitch of the visual field topbackward by an angle θ around a center of rotation at the eye of an observer in (b) produces an identically located retinal image as the one produced by elevating the direction of gaze by θ in an erect visual field in (a). (c) and (d) Setting the pitch of the visual field topforward by an angle θ around a center of rotation at the eye of an observer in (d) produces an identically located retinal image as the one produced by depressing the direction of gaze by θ in an erect visual field in (c).

mension, it is best dealt with as a rotation of perceived directional coordinates around an axis at eye level in the frontal plane of the observer relative to coordinates centered at the eye (Post & Welch, 1996; Li & Matin, 1999).

An analysis of the visual stimulus in conjunction with experiments demonstrating that the elevation of VPEL for a given set of conditions is essentially independent of head orientation and the orientation of the eye in the orbit (Li & Matin, 1991a,b, 1993; Matin & Li, 1995a) suggests that the VPEL settings are controlled by a neural loop that evolved as a means of maintaining the stability of the perception of elevation of visual objects and locations ('perceptual constancy') regardless of eye and head movements (Matin & Li, 1994c). For example, if, with the eyes fixed in the stationary head of an observer, the visual field is pitched topforward around an axis centered on the horizontal line between the two eyes, the change in image position and orientation on the retina will be essentially identical to that produced by lowering the eyes by the same angle with the head and visual field stationary (Fig. 2). Many of the significant issues regarding the basis for SDSPVP relate to the mechanisms by which feedback from the various extraretinal influences occurs. Experimental variation of the orientation of the visual field has allowed us to break into the loop controlling VPEL and forced the occurrence of the systematic perceptual and manual mislocalizations.

2. VPEL and the influences of pitched-from-vertical lines and roll-tilted lines

The influence of visual pitch on the elevation of VPEL is only a little less when an observer views a visual field consisting of either one or two pitched-from-vertical[3] inducing lines in otherwise total darkness ('1-line stimulus' or '2-line stimulus'; Fig. 1b–d) than when viewing the complexly-structured, well-illuminated visual field of the pitchroom. Thus, the influence of the orientation of a long 1-line stimulus is 84% as large as that of the full pitchroom, and the influence of a long 2-line stimulus is 89% as large as that of the full pitchroom (Matin & Li, 1992a,b, 1994a,b,c). Systematic variation of the pitch of a visible surface in front of the observer that contains as little as a single, dim, 25°-eccentric, long, pitched-from-vertical line, pitched over the range from − 30° (topbackward) to + 20° (topforward) generates a near linearly related change of the elevation of VPEL that extends from approximately − 19° to + 7° (Matin & Li, 1994a). Results of measurements with monocular and binocular viewing in the complex visual environment of the pitchroom are indistinguishable (Stoper & Cohen, 1989; also compare re-

---

[3] A 'pitched-from-vertical line' is a line that becomes vertical when the plane on which it lies is rotated around the pitch axis to an erect orientation; a 'pitched-only plane' is any plane that is perpendicular to the median plane of the observer.

sults in Matin & Fox, 1989 with results in Matin & Li, 1992b), indicating that stereovision is not necessary and may not be involved. However, dichoptic transfer of adaptation of the influence is substantial, both in the complex environment and in an environment reduced to a 2-line pitched-from-vertical stimulus in darkness (Matin & Li, 1995a), indicating that the system processing the influence is not exclusively monocular. Interestingly, although our early views were that the mechanisms controlling the perception of pitch and the influence of pitch on VPEL are causally related, although a large number of perceptual psychologists (and others) who have viewed the pitchroom have offered similar views, and although the magnitude of perceived visual pitch varies systematically with the magnitude of the physical pitch as does the deviation of VPEL from TEL, three different sorts of evidence have indicated that the mechanism controlling the perception of elevation and the mechanism controlling the perception of pitch are independent (Servos et al., 1995; Li & Matin, 1996, 1998; Hudson, Li, & Matin, 1997, 2000). The concern of the present article is with the perception of elevation and not at all with the perception of pitch. Some relations between the perception of pitch of a visual field and the perception of elevation of visual objects are dealt with elsewhere (Li & Matin, 1996, 1998; Hudson et al., 1997, 2000).

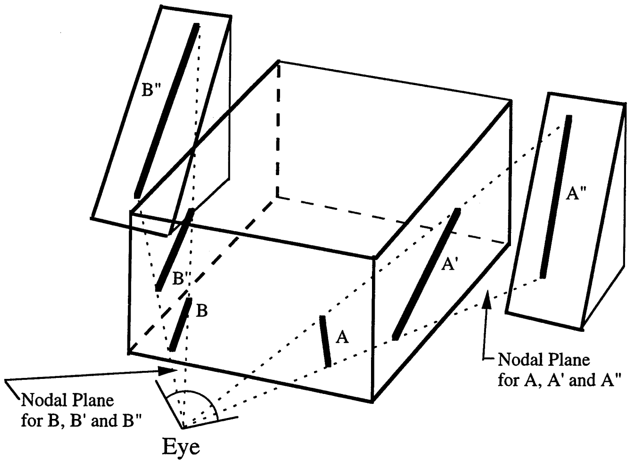

Fig. 3. (a) The observer's eye is shown viewing a visual field that contains lines A, A′, and A″, each in a differently oriented plane in space, although all three arise from the same nodal plane; no two of the three lines are parallel. All three produce stimulation at the identical retinal orientation. Since the lengths of each of the three terminate at the same sides of the triangle defining the nodal plane (small dashed lines) we also refer to them as spanning the same nodal triangle. Similar relations hold for lines B, B′, and B″ and their nodal plane and nodal triangle. Lines A′ and B′ are parallel as are A″ and B″, but A and B are of equal and opposite orientations relative to a plane of symmetry through the median plane of the eye that is perpendicular to the plane containing A and B (i.e. A and B are bilaterally symmetrical).

Although the significant stimulus change that generates the changes in elevation of VPEL described above is the change in the pitch of the visual field, the VPEL changes do not depend uniquely on the presence of visual pitch: An oblique line in the frontoparallel plane that falls within the same nodal plane (Fig. 3) of a monocularly-viewing observer as does a pitched-from-vertical line exerts an influence on VPEL that is indistinguishable from that of the pitched-from-vertical line (Li & Matin, 1996). Thus, the particular depth or variation in depth of the plane of origin of a line stimulus is not important for the VPEL discrimination. This generalization is supported by a number of additional experiments and calculations that have demonstrated that the influence of a line on the elevation of VPEL is independent of retinal gradients of blur, image width, and intensity (all of these gradients are normal concomitants of variation in depth [i.e., pitch]), and of accommodation, or a stimulus arising from accommodation (Matin & Li, 1994a).

A number of experiments have been carried out in which the influence on the elevation of VPEL has been measured with 1-line stimuli of different lengths and orientations whose origin has been in pitched-only (see footnote 3) or erect planes, and with 2-line and 3-line combinations of these lines (Matin & Li, 1992a,b, 1994a,b,c, 1995a, 1999a, 2000; Li & Matin, 1996, 1997b). The simplicity of the main features of the results and the centrality of their dependence on line orientation encourages the view that the influence has its origin in the properties of individual orientation-selective units in primary visual cortex and their combinations. The model we describe here for the VPEL discrimination makes use of some of the known properties of these units and is fitted to several sets of experimental results that permit us to examine the model under conditions in which the parameters related to deviations of gaze from the median plane and inducing line eccentricity are constrained and can be treated as fixed constants. The present version of the model is intended to characterize the neural mechanism by means of which the total visual influence is assembled from a set of stimulus elements. In a subsequent article (in preparation) we will break out the parameters of gaze direction and inducing line eccentricity for full treatment; Section 7 below describes some of the complexities that variation of these parameters introduce and that will be modeled in the subsequent article.

The main aspects of the psychophysical results with single lines and 2-line pitched-from-vertical combinations that we relate to the model in the present article were typically measured with lines at 25° horizontal eccentricity lying in planes whose pitch ranged from -30 to $+30°$; the subjects were erect, viewed the visual field monocularly, and directed their gaze within a midsagittal plane of the viewing eye. The essential features of these results are displayed in the figures which follow along with their fits to the model. They include the following: (a) The influence of a single line on the elevation of VPEL is bilaterally symmetric; i.e., individual lines with mirror symmetry on opposite sides of the median plane exert identical influences on the elevation of VPEL, and antisymmetric lines relative to a plane of symmetry in either the frontoparallel plane or median plane exert equal and opposite influences (Matin & Li, 1992a,b, 1994a,b,c, 1999a, 2000). (b) The growth of the influence on VPEL is a negatively accelerated function of the length of the one-line stimulus, with stable space constants for individual subjects that differ among subjects in the range between 10° and 20°. The asymptote of this VPEL-versus-line-length function increases nearly linearly with the deviation of the orientation of the pitched-from-vertical line from an erect orientation (Li & Matin, 1991a; Matin & Li, 1994b). (c) The influence of two simultaneously-presented long lines with any combination of orientations at bilaterally symmetric horizontal eccentricities is close to the average of their two individual influences when presented individually (Matin & Li, 1999a). (d) Two long, parallel, bilaterally symmetric, pitched-from-vertical (including zero-pitched) lines of identical length presented simultaneously generate an influence that is slightly greater than the influence of a single line of the same total length as the 2-line combination (Matin & Li, 1994b). (e) The influence of two simultaneously-presented short lines of identical length with any combination of orientations presented at bilaterally symmetric horizontal eccentricities is equal to the sum of their influences when presented individually (Matin & Li, 1989, 2000). (f) The nearlinearity of the VPEL-versus-pitch function leads to the fact that all of these results are well-represented by the same relation with only a change of the slope constant b that depends on line length (Matin & Li, 2000):

$$\mathbf{V}(\theta_l, \theta_r) = a + b[\mathbf{V}(\theta_l) + \mathbf{V}(\theta_r)] \tag{1}$$

where θ_l and θ_r equal the pitches of lines to the left and right of the median plane, respectively, and a and b are the best-fitting linear constants to the relation between VPELs for 1-line and 2-line stimuli (Fig. 5). For the slope constant $b = 1.00$, Eq. (1) predicts that $\mathbf{V}(\theta_l, \theta_r)$, the VPEL for the 2-line stimulus, equals the algebraically additive linear sum of the influences of the two individual lines. For $b = 0.50$, Eq. (1) predicts that the VPEL for the 2-line stimulus is the average of the influences of the two individual lines. The experimental results for short lines manifest linear summation (12°-long lines, best-fitting value of $b = 0.99$); the results for long lines manifest nearaveraging (64°-long lines, $b = 0.61$).

3. Bilateral symmetry, nodal planes, and the projection sphere

Two assumptions have been universal in the use of orientation-selective neural units for modeling visual pattern perception and visual movement perception, as well as in previous modeling of the perception of orientation within a frontal plane: (a) we normally perceive physically parallel lines as possessing the same orientation; (b) parallel lines act similarly on the visual nervous system to form perceptual groups. The theoretical treatment of line orientation by these approaches to perception has generally assumed a coordinate framework in which the coordinates are centered on surfaces or objects or locations in the world independently of the observer; even on occasions in which theoretical work has employed a projection plane between the visual field and the observer, the location of the origin of coordinate values for directions and distances within the plane has been arbitrary. This cluster of assumptions ('grouping-by-parallels') appears to have considerable validity for the perception of visual patterns and at least for some visual movement as well as for some other discriminations. However, grouping-by-parallels cannot be employed as the basis for modeling the influences on the elevation of VPEL that results from induction by lines. As noted above, lines on opposite sides of the median plane must be bilaterally symmetric in order to exert influences of the same sign and magnitude on the elevation of VPEL. Although parallel pitched-from-vertical lines are indeed bilaterally symmetric, and exert equal influences on the elevation of VPEL, other bilaterally symmetric lines are not generally parallel (e.g. lines of equivalent pitch to parallel pitched-from-vertical lines — roll-tilted lines within a frontoparallel plane — are not parallel; see Figs. 3 and 4). Nevertheless, although not parallel, such bilaterally symmetric roll-tilted lines exert identical influences on the elevation of VPEL. These geometric connections are clarified most readily by an example that can be referred to Fig. 4: an oblique 1-line stimulus in the frontoparallel plane, turned 15° counterclockwise-from-vertical and lying to the left of the observer's median plane (Fig. 4b), exerts an influence on VPEL that is identical to the influence exerted by the 15°-clockwise-rotated mirror-symmetric line on the right side of the observer's median plane. Each of these two nonparallel and bilaterally symmetric, oblique lines generates an upward deviation of the VPEL setting. But the two parallel pitched-from-vertical lines within the nodal planes containing these oblique lines are bilaterally symmetric also (Fig. 4a), and all four of these lines exert identical upward influences on the elevation of VPEL (Li & Matin, 1996). Similar relations hold for a clockwise-rotated line on the left side and a counterclockwise-rotated line on the right side of the median

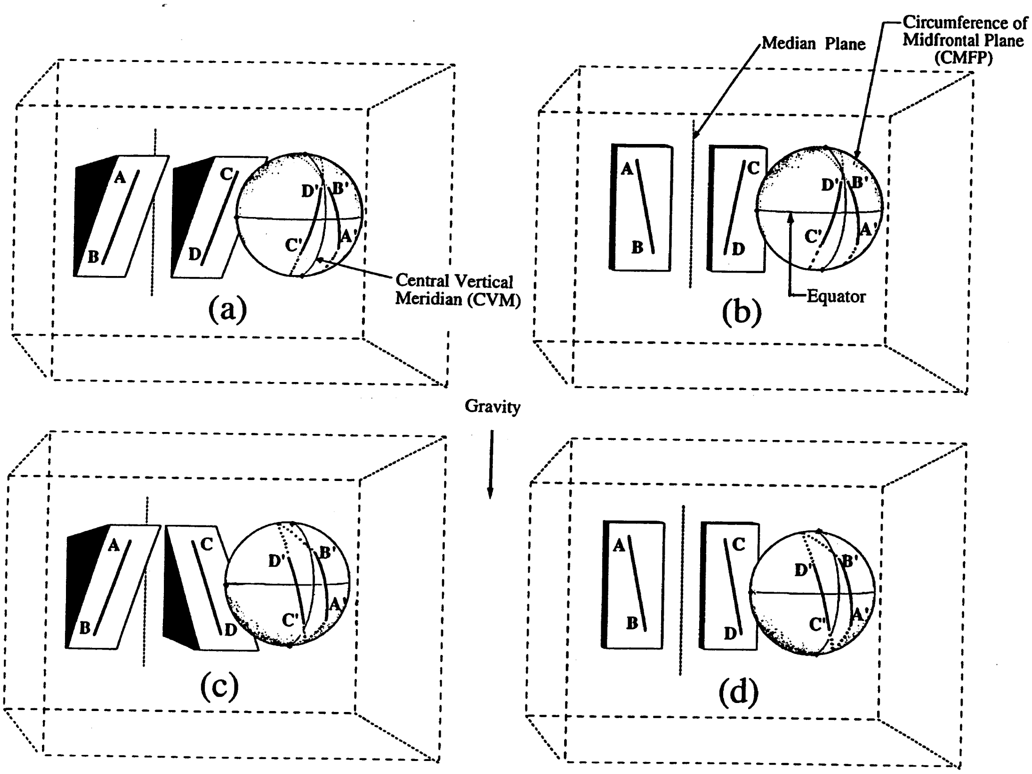

Fig. 4. Projection spheres centered on the eye of the erect observer in primary viewing position viewing a 2-line visual field. The central vertical meridian (CVM) is the great circle that corresponds to the median plane of the eye of the observer; the circumference of the midfrontal plane (CMFP) is a frontoparallel section through the sphere; the equator is horizontal at the observer's eye level. In each of the four panels the two lines are at equal horizontal eccentricities on opposite sides of the median plane. Each of the two pairs of panels [(a)/(b), (c)/(d)] displays the identity of central projections on the projection sphere from two pitched-from-vertical lines on pitched-only plane(s) with two oblique lines on an erect frontoparallel plane. The two lines in (a) are parallel and lie in a single pitched-only plane; the two lines of 'equivalent pitch' in its erect-plane counterpart in (b) are mirror symmetrical. The two lines in (c) lie in pitched-only planes of equal and opposite pitch; the two lines in its erect plane counterpart in (d) are parallel. Systematically changing the pitch of the plane containing a line from topbackward to topforward produces a linearly related change in the intersection of the great circle projection of the line with the CVM.

plane (both arising from the frontoparallel plane) and the parallel, topbackward, pitched-from-vertical counterparts from their nodal planes; all four of these lines generate downward deviations of VPEL of indistinguishable magnitude.

The grouping-by-parallel assumptions emphasize relations among parts of external objects and among parts of the visual field without specific reference to the observer, and so, of course, the employment of object-centered coordinates that invariably accompany their use gives the median plane of the observer no special position, certainly not one in which the significance of a given line orientation for a perceptual discrimination reverses when that line is translated across the median plane. Nor, as noted above, is such bilateral symmetry an inherent property of the projection plane that is employed so frequently to represent visual stimuli. However, it is an inherent property of imaging on the projection sphere (Fig. 4) where the pinhole pupil is centered within the projection sphere in a plane that is orthogonal to the line of sight through the 'fovea', and the central vertical meridian (CVM) is a natural axis for bilateral symmetry, and, it is, of course an inherent property of imaging on the eye (to the extent that the sphere can serve as an approximation to the eye). Since the model in the present article is developed for the case with gaze restricted to the median plane, the bilateral symmetry is with respect to a line of symmetry in the retina through the fovea: parallel lines stimulating the two halves of the retina at equal but opposite eccentricities exert equal and opposite influences on VPEL whereas lines that stimulate bilaterally symmetric orientations on opposite sides of the retina exert the same influences on VPEL.

4. Neural model for VPEL

Our main purpose in constructing the present model was to develop a quantitative account for the visual influence on VPEL that would deal with the results of the experimental work in which the main parameters of the visual line stimulus were systematically manipulated. The results of the modeling work demonstrate

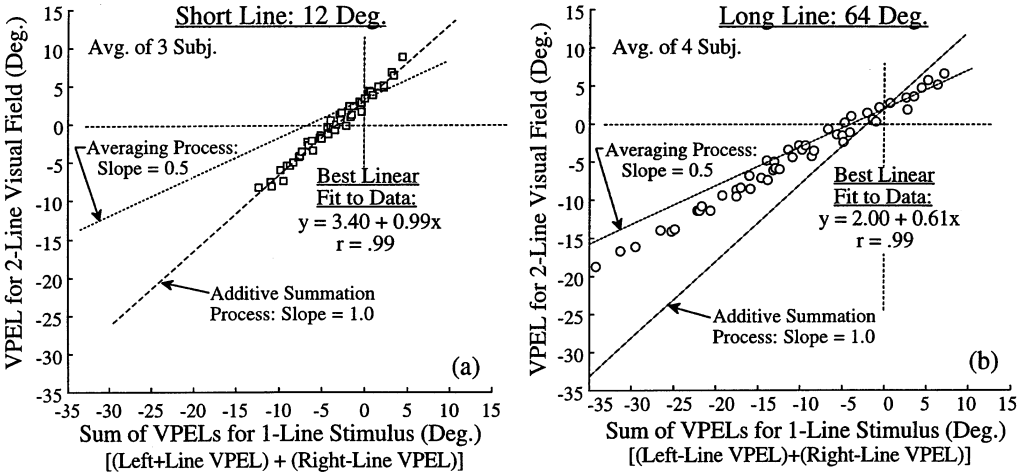

Fig. 5. The figure displays the results of two experiments (Matin & Li, 1999a, 2000) in each of which 49 2-line pitched-from-vertical combinations were employed. Each 2-line combination contained a line 25° to the left of the median plane and a second line 25° to the right of the median plane. Each of seven orientations of the line on the left of the median plane (− 30°, − 20°, − 10°, 0°, 10°, 20° and 30°) was combined with the line on the right of the median plane at one of the seven orientations to constitute the 49 combinations. The results in panel (a) are for 12°-long lines, those in the panel (b) are for 64°-long lines. Each data point is the average of four method-of-adjustment trials on each of three subjects in (a) and four subjects in (b). The ordinate displays the VPEL for the 2-line stimulus plotted against the sum of the VPELs of the two constituent one-line stimuli measured separately. The slopes of the two theoretical straight lines shown in each panel are those that would result if the total visual influence contributing to the 2-line VPEL was the sum of the contributions of the two constituent lines ('additive summation process') and the average of the VPELs of the two constituent lines ('averaging process'), respectively.

that, with reasonably simple, realistic neural circuitry, a neural computation over a very large area of the visual field is capable of generating the total visual influence on the elevation of VPEL. In the present article, we restrict our attention to experiments with the gaze of the erect stationary subject constrained to the median plane and with inducing line(s) of variable length and orientation at only two locations: at true eye level 25° to the left and/or right of the median plane. As a consequence of these experimental constraints on head and eye position combined with the constraints on stimulus line eccentricity, the contributions of extraretinal signals regarding head and/or eye position can be treated as fixed parameters and their influences lumped into a single constant that is linearly additive with the visual influence: We have referred to this lumped parameter as the contribution of the body-referenced mechanism[4] (Matin & Fox, 1989) and will discuss some matters relating to it further in Sections 5 and 7 below.

Fig. 6 contains an outline of the present model that accounts for the quantitative properties of the processing of the visual influence on the visual perception of elevation. The approach we take assumes that the visual influence is organized in stages within the visual system prior to its combination with influences from the body-referenced mechanism. The model consists of three serially ordered stages (Fig. 6a) that carry out its three main operations in the transformation between the visual input (stimulus lines) and the output (VPEL discrimination): producing orientation-sensitivity, integrating the resulting opponent orientation signals from oriented line stimuli on both sides of the visual field to yield the visual influence on the elevation of VPEL, and combining the total visual influence with the lumped influence from the body-referenced mechanism. The model assumes an erect, stationary, monocularly-viewing observer with gaze directed within the median plane at true eye level.

4.1. The first stage of the model

For purposes of modeling the induction-by-lines of changes in the elevation of VPEL, an assumption of bilateral symmetry must replace the assumption of grouping-by-parallels as an organizational principle both with regard to influences on the perception of elevation and with regard to the way in which the outputs of orientation-selective neural units contribute to perception. This requires a reversal of the sign of the influence of signals from units in V1 with identical sensitivity to orientation on opposite sides of the median plane (and thus in opposite hemispheres).

In the first stage (Fig. 6) two classes of orientation-sensitive neural units in V1 respond to the individual

---

[4] The term 'body-referenced mechanism' was introduced (Matin & Fox, 1989) to refer to the combination of all influences on VPEL that arise from sources other than the visual field extrinsic to the target employed to measure VPEL itself. It is intended to include extraretinal eye position information (EEPI), extraretinal head orientation information (EHOI; including information regarding the head relative to the body and from the head relative to gravity), other affects of gravity on the body, pressure cues from the surfaces of the body, joint receptors, and the vestibular organ.

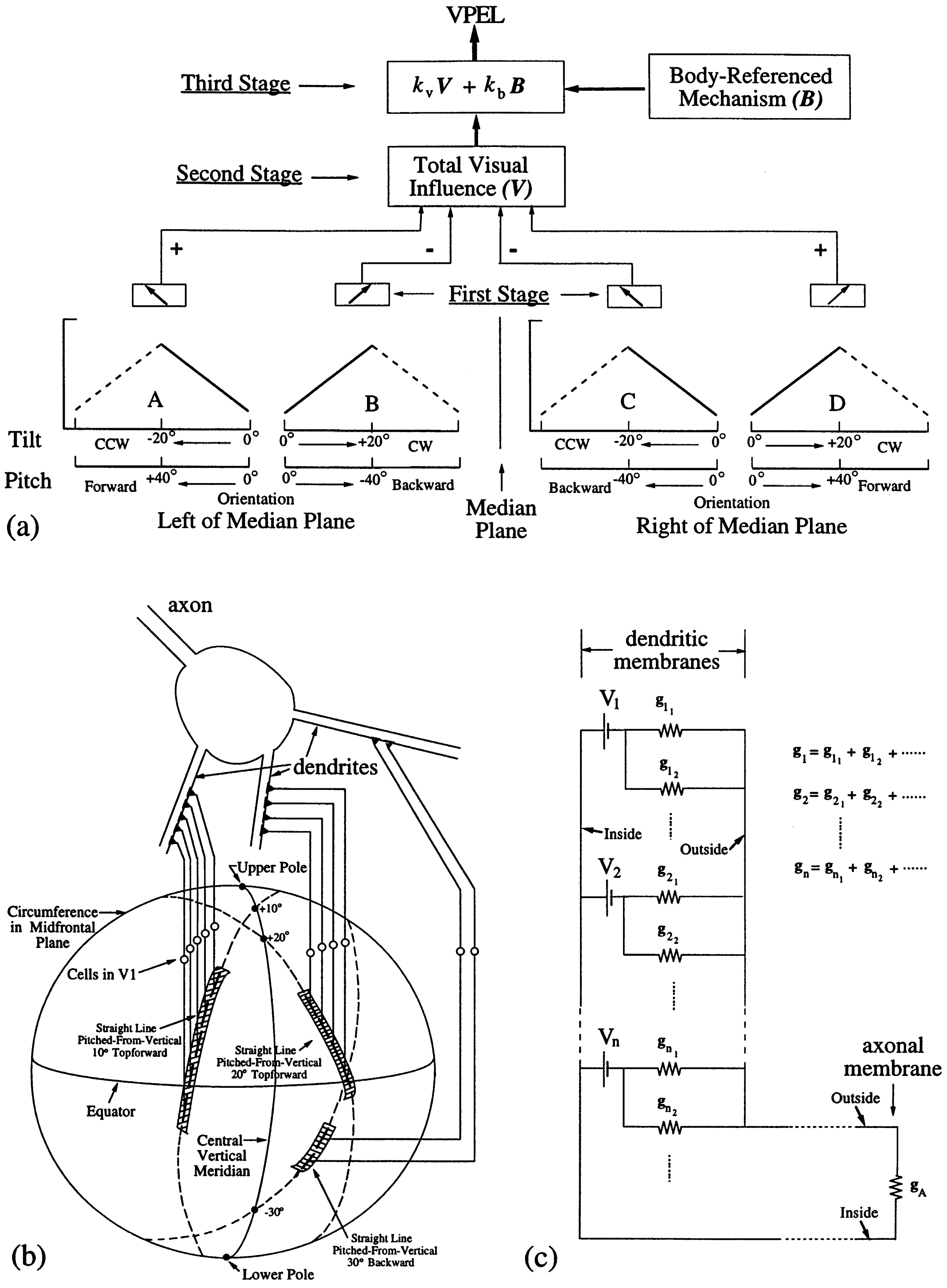
VPEL
Third Stage
$k_v V + k_b B$
Body-Referenced Mechanism (B)
Second Stage
Total Visual Influence (V)
+
-
-
+
First Stage
A
B
C
D
Tilt
CCW -20° 0°
0° +20° CW
CCW -20° 0°
0° +20° CW
Pitch
Forward +40° 0°
0° -40° Backward
Backward -40° 0°
0° +40° Forward
Orientation
Left of Median Plane
Median Plane
Orientation
Right of Median Plane
(a)
axon
dendrites
Upper Pole
+10°
+20°
Circumference in Midfrontal Plane
Cells in V1
Straight Line Pitched-From-Vertical 10° Topforward
Straight Line Pitched-From-Vertical 20° Topforward
Equator
Central Vertical Meridian
-30°
Straight Line Pitched-From-Vertical 30° Backward
Lower Pole
(b)
dendritic membranes
V_1
g_{1_1}
g_{1_2}
Inside
Outside
V_2
g_{2_1}
g_{2_2}
V_n
g_{n_1}
g_{n_2}
$g_1 = g_{1_1} + g_{1_2} + \cdots$
$g_2 = g_{2_1} + g_{2_2} + \cdots$
$g_n = g_{n_1} + g_{n_2} + \cdots$
axonal membrane
Outside
g_A
Inside
(c)

Fig. 6.

stimulus lines on each side of the median plane, one for topforward pitch (A, D) and a second for topbackward pitch (B, C). It is assumed that each local region of the visual field is served by many such units with overlapping receptive fields. The geometric relations between orientations of pitched-from-vertical and roll-tilted lines within the nodal plane (Figs. 3 and 4) require that units processing pitched-from-vertical lines from planes with topbackward pitch be sensitive to clockwise roll-tilt of line orientations on the left side of the median plane but to counterclockwise roll-tilt on the right side of the median plane. The reverse arrangement is required for units responsive to pitched-from-vertical lines from planes with topforward pitch: these units must be sensitive to line orientations with counterclockwise roll-tilt on the left side of the median plane but clockwise roll-tilt on the right side of the median plane. Stage 1 units processing topbackward pitched-from-vertical lines on both sides of the median plane generate negative signals (B, C, Fig. 6a); units processing topforward pitched-from-vertical lines generate positive signals (A,D, Fig. 6a). Thus, stage 1 units with sensitivity to identical roll-tilt orientations on the two sides of the median plane produce opposite-signed outputs as required above; units on the same side of the median plane that are sensitive to oppositely directed roll-tilt orientations produce opposite signed responses.[5] The signals resulting from the processing of topbackward and topforward lines drive the nerve impulse frequency at the output of stage 2 neural units down and up, respectively, relative to a baseline value.

Sensitivity of each stage 1 neural unit peaks at roll-tilts of 20° with symmetrical rolloffs to zero at 0° and 40°. The model employs linear sensitivity profiles for the neural units. Although V1 receptive fields are sometimes portrayed as Gaussian and sometimes as linear, we know of no work that provides a clear reason for deciding on the best representation. The fit of theory to data here is not influenced significantly by fitting with Gaussians. We assume that the outputs from a large number of V1 units with common orientation/response characteristics that are stimulated by a given line all terminate on a dendrite of a neuron in stage 2 where integration across outputs from stage 1 units takes place. Consistent with known receptive field sizes (Hubel & Wiesel, 1974, 1977) most V1 units are assumed to be responsive only to a small segment of one of the stimulus lines (1° to 3°**)**. However, the responses of at least some units in primary visual cortex increase with increasing line length up to considerably larger lengths and could provide a significant contribution to the output of stage 1 (see Sections 6 and 8).

4.2. The second stage of the model

The second stage of the model combines the signals due to stimulation from all orientation-sensitive neural units processing topforward and topbackward pitch (and roll-tilted lines of equivalent pitch) on both sides of the median plane, producing an output appropriate for an opponent-process mechanism.[6] Thus, for example, an increase in the response from a dendrite receiving neural units of class A (Fig. 6a) along with a decrease in the response of identical magnitude from a dendrite receiving neural units of class C leaves the output of the total visual influence on VPEL unchanged, in correspondence with the fact that VPEL remains constant as a result of an increase in topforwardness of one line of a 2-line stimulus together with an increase in topbackwardness of the second line.

The second stage is based on the classical view of the single neuron as an integrating device for combining the influences of a number of inputs to a set of *n* dendrites (Eccles, 1957; Shepherd, 1998): the consequence of stimulation by a line is the generation of a signal in a set of stage 1 neurons that are presynaptic to

---

[5] The same set of modeling objectives would be accomplished here by assigning negative and positive signs to the outputs of units A and B, respectively, and inserting sign-inverters between their outputs and the inputs to stage 2.

[6] We call attention to the fact that in Fig. 6 V1 units, which serve both sides of the median plane and receive their signals from opposite sides of the retina, are connected to different dendrites on the same neuron. Our attempt here is to display only the features of a neural network that are significant for the processing of visual input as it influences VPEL, and the direct connection displayed is not meant to imply that there are no intervening synapses between V1 output from either side and the subsequent collecting neuron (see Section 6 regarding this matter).

Fig. 6. The three panels together provide an outline of the model for generating the elevation of visually perceived eye level (VPEL). Panel (a) contains a flow diagram of the three stages in which the first stage contains two classes of orientation-sensitive units on each side of the median plane. The second stage combines signals from all four classes of stage 1 units, and its output, containing the total visual influence, is sent to the third stage where it is combined with influences from the body-referenced mechanism. The transform between visual pitch, θ, of a plane that contains a pitched-from-vertical line at a horizontal eccentricity, μ, and the roll-tilt, ρ, of a line within a frontal plane that possesses the equivalent pitch to that of the pitched-from-vertical line is $\rho = \arctan(\tan \mu \times \sin \theta)$ (see Appendix in Li & Matin, 1996, for derivation and details). Panel (b) shows the images of three straight lines of different lengths and orientations on a projection sphere (see Fig. 4), each of which stimulates several orientation-selective neurons. The total visual response at the initial segment of the axon of the integrating neuron (‘total visual influence’) is the result of responses produced by all of the stimulated neural units. Panel (c) shows the electrical circuit representation of the integrating neuron being stimulated by $\boldsymbol{n}$ lines; each branch represents the signal resulting from stimulation by a different line stimulating a different dendrite. See text for further detail.

the integrating neuron; the two significant postsynaptic consequences in the dendrite on which the presynaptic input impinges are the generation of changes in conductance of the dendritic membrane and the generation of changes in dendritic membrane potential. The integration of the currents from the different stimulated dendrites takes place at the initial segment of the axon where action potentials are initiated. Fig. 6 sketches this arrangement showing inputs from several stimulus lines on to several dendrites, each mediated by a number of stage 1 neurons. Fig. 6c represents the significant steady state electrical changes across the postsynaptic membranes of dendrites on a second stage neuron that are the effects of stimulation by the $\boldsymbol{n}$ stimulus lines: With $i = 1, 2, \ldots, \boldsymbol{n}$, $\mathbf{V}_i$ represents the change in membrane potential in dendrite i that is a consequence of stimulation by the set of presynaptic neurons whose receptive fields are themselves stimulated by line i. Since the synapses involving different presynaptic neural units terminating on a given one of the dendrites can be treated as being arranged electrically in parallel, their conductances can be assumed to add linearly, and we thus assume that the net postsynaptic conductance change, g_i, in a single dendrite, represented by a single branch in Fig. 6c, is proportional to the length of the stimulus line. Consistent with reasonable assumptions about the relation of electrotonic space constant and dendritic length, we also assume that the membrane on a given dendrite is isopotential, and thus represent the potential change resulting from all EPSPs from the different synapses on dendrite i by the single value $\mathbf{V}_i$ ($\mathbf{V}_i$ is the deviation of membrane potential from the reversal potential) in series with g_i ($= g_{i_1} + g_{i_2} + \cdots$; Fig. 6c). The longitudinal extracellular and intracellular electrical resistances between the postsynaptic membrane receiving stimulation and the initial segment of the axon are assumed to be negligible relative to the transmembrane resistances at the postsynaptic membrane and at the axon's initial segment. Since the concern here is only with the steady-state, transmembrane capacitances are neglected.[7] The threshold conductance at the initial segment of the axon, g_A, is assumed to remain constant.[8] The shunting inherent in the circuit (Fig. 6c) among branches does not control the change in postsynaptic conductance of the individual synapses; chemical synapses are assumed. Although Ohm's-law simplicity holds in each branch of the model's network, the shunting of current from one dendrite (one branch in the circuit) to others affects the driving potential in the other active branches. This change in driving potential at the synapse of an affected branch may be considered as feedback through shunting of the electrical flow from one branch on to others, and is an inherent consequence of differences between the voltages in the circuit in Fig. 6c. Such shunting is of more significance at higher stimulus levels (longer stimulus lines) where it is involved in the shift from linear summation to nearaveraging as we describe below. Although the model assumes shunting in branches receiving stimulation only, such shunting will also occur at nonstimulated branches as well, a background effect that we can neglect here. The solution to the system of equations governing the flow of current in the circuit of Fig. 6c is obtained from the set of n loop equations

$$
\begin{aligned}
&\mathrm{V}_2 - \mathrm{V}_1 = \mathrm{I}_1/(g_1 + g_2) - \mathrm{I}_2/g_2\\
&\mathrm{V}_3 - \mathrm{V}_2 = -\mathrm{I}_1/g_2 + \mathrm{I}_2/(g_2 + g_3) - \mathrm{I}_3/g_3\\
&\mathrm{V}_4 - \mathrm{V}_3 = -\mathrm{I}_2/g_3 + \mathrm{I}_3/(g_3 + g_4) - \mathrm{I}_4/g_4\\
&\cdots\cdots\cdots\\
&\cdots\cdots\cdots\\
&\mathrm{V}_n - \mathrm{V}_{n-1} = -\mathrm{I}_{n-2}/g_{n-1} + \mathrm{I}_{n-1}/(g_{n-1} + g_n) - \mathrm{I}_n/g_n\\
&-\mathrm{V}_n = -\mathrm{I}_{n-1}/g_n + \mathrm{I}_n/(g_n + g_\mathrm{A}) \qquad (2)
\end{aligned}
$$

in which $\mathrm{I}_1, \mathrm{I}_2, \ldots, \mathrm{I}_n$ are the currents in dendrites 1, 2,..., n resulting from the EPSPs in the branches that give rise to $\mathrm{V}_1, \mathrm{V}_2 \cdots \mathrm{V}_n$. Since the solution will only be applied here to cases in which the $\boldsymbol{n}$ simultaneously-presented lines are of equal length, the expressions can be considerably simplified by assuming that the g_i are all equal to the same value, g_S. The assumption of proportionality between conductance change and line length was itself based on assuming that increasing line length brings in more stage 1 neural units with the same sensitivity to orientation whereas the outputs of all of the units serving a single line are themselves identical (reasonable amounts of variability among neural units, both in sensitivity to orientation and overall, will have negligible influences on the predictions we make here); increase in line length has no influence on the response of those stage 1 units with small receptive fields whose response is already saturated by the shorter line. The solution of the system in Eq. (2) for I_n is

---

[7] Transmembrane capacitances are not included in the present treatment since the subject can be assumed to be at steady state for all of the experimental results fitted to the model below. The model (with capacitances included) is inherently capable of treating the effects of temporally varying stimulation, but appropriate experimental work on the matter is lacking. Some information on the growth and decay of the influence on VPEL with time following stimulus onset and offset is available (Matin & Li, 1995b), but is of particular interest regarding adaptation of VPEL rather than the influence of transient or temporally varying stimulation per se.

[8] The conductance g_A represents the value at which regenerative changes begin to take place at the axon's initial segment, i.e. the threshold for spiking in the nerve impulse. An excitability cycle is, of course, associated with the nerve impulse, as are systematic temporal variations of the major conductances and differences in threshold for a spike within trains of nerve impulses that differ in impulse frequency. We have not attempted to include such variations here explicitly. These variations, along with separate representation of the different ionic conductances, will need to be included in more detailed developments and in treatments of psychophysical experiments that are more directly aimed at such neurophysiology.

$$\mathrm{I}_n = \frac{\sum_{i=1}^{n} \mathrm{V}_i}{(1/g_\mathrm{S}) + n(1/g_\mathrm{A})}. \tag{3}$$

Thus, we have as the voltage change, $\mathrm{V_A}$, at the initial segment of the axon,

$$\mathrm{V_A} = \frac{\sum_{i=1}^{n} \mathrm{V}_i}{n + (g_\mathrm{A}/g_\mathrm{S})}. \tag{4}$$

For small enough values of g_S so that the ratio $g_\mathrm{A}/g_\mathrm{S}$ is sufficiently large relative to n, $\mathrm{V_A}$ approximates the sum of its inputs, that is, each branch acts as a high impedance current source sending current into a lower impedance axon that sums their contributions linearly:

$$\mathrm{V_A} \approx \frac{\sum_{i=1}^{n} \mathrm{V}_i}{(g_\mathrm{A}/g_\mathrm{S})}; \tag{5}$$

thus, adding the nth input to $n-1$ other inputs increases the output $\mathrm{V_A}$ by $\mathrm{V}_n/(g_\mathrm{A}/g_\mathrm{S})$. For large enough values of g_S so that the ratio $g_\mathrm{A}/g_\mathrm{S}$ is sufficiently small relative to n, the circuit approximates the weighted average of its inputs, that is

$$\mathrm{V_A} \approx \frac{\sum_{i=1}^{n} \mathrm{V}_i}{n}; \tag{6}$$

thus, although for $\boldsymbol{n}$ equally potent long lines, adding the nth input to $n-1$ inputs reduces the relative influence of each the addition of the $\boldsymbol{n}$th line does not affect $\mathrm{V_A}$.

Assuming that postsynaptic voltage V_i due to stimulation by a 1-line stimulus increases linearly with pitch θ_i (or with its equivalent pitch), that postsynaptic conductance g_S increases linearly with stimulus line length, $\boldsymbol{l}$, that nerve impulse frequency increases linearly with $\mathrm{V_A}$, that the visual influence, $\boldsymbol{V}$, increases linearly with nerve impulse frequency, substitution in Eq. (4) yields

$$\boldsymbol{V} = \frac{k_1 \sum_{i=1}^{n} \theta_i}{\boldsymbol{n} + (k_2/\boldsymbol{l})} \tag{7}$$

where k_1 (in degrees visual angle/degrees pitch) is the constant of proportionality between the visual influence and pitch, k_2 (in degrees visual angle) is equal to g_A divided by the constant of proportionality relating line length and g_S, and $\boldsymbol{n}$ equals the number of stimulus lines in the visual field, one for each of the n active dendrites. From Eqs. (5)–(7) then, the model acts as a summing device for small lines and as a device that generates the average of the influences of its $\boldsymbol{n}$ inputs for long stimulus lines.[9]

4.3. The third stage of the model

The model characterizes the influence of the visual field on the elevation of VPEL for purposes of fitting the results of experiments in which the direction of gaze

---

[9] The centerpiece of the second stage of the present model is the variable postsynaptic conductance. Such a conductance variation was first employed as a basis for a model that predicted the results of psychophysical experiments involving temporally varying stimulation, including the effects of the level of light and dark adaptation on temporal resolution and integrating ability during intensity discrimination of flashes of different durations and intensities viewed against steady backgrounds over a wide range of luminances, and on the detection of flicker for square wave or sinusoidally flickering stimuli over a similarly wide luminance range (Matin, 1968). In that case the main effect of the variable conductance that was of interest was the correlated production of variation in gain and time constant, and it was reasonable to assume that the conductance variation took place in the retina. The employment of the conductance changes as a parameter in the neural modeling of psychophysical phenomena and neural processes themselves has become fairly common since then as it has in the modeling of neural processes not simply based on sensory stimulation. In the present case two sorts of evidence strongly support the likelihood of mediation at cortical loci beyond V1 for the conductance changes (also see Section 6): (a) the summation of influences on VPEL from individual lines that we model here extends across the two hemispheres; (b) 85% dichoptic transfer of VPEL adaptation across the two hemispheres is measured with either the full pitchroom or the 2-line pitched-from-vertical stimulus (Matin & Li, 1995b). The present model and the 1968 model were devised for treating different segments of visual perception, and additional useful perspective can be derived from noting three other significant differences between th two: (a) The present model computes its result by applying Eq. (8) to a set of parallel inputs whereas the earlier model consisted of a serial n-stage filter with n identical rc stages that responded to a single input. (b) Whereas the conductance variation in the earlier model was output-controlled, in the present model the conductance variation is entirely input-controlled, the result of a feedforward process. Nevertheless, current from one branch influences the driving potential in other branches (shunting feedback) and its consequences become more significant for longer lines where it contributes significantly to generating an output that is nearly equal to the average of the inputs. That such feedback is a possible basis for averaging can be seen from the fact that the effect of each of the $n-1$ inputs is reduced by the addition of the nth input. In addition, however, the only variation of the present model that does not run into serious disagreement with the results for either short-line or long-line experiments is one in which $\boldsymbol{n}$ in the divisor of Eq. (8) acts on the contribution of all individual lines. Several versions in which $\boldsymbol{n}$ in the divisor is restricted to the number of lines in a single channel in a multichannel version of the present model (i.e. different channels for topforward and topbackward pitch) fail; only if the action of $\boldsymbol{n}$ is distributed across all lines does the model not generate significant disagreement with results. (c) The variation in conductance in the earlier model was generated by variation in brightness-produced adaptation level whereas in the present model it is a consequence of variation in line length. Brightness variation is of considerably less significance for egocentric spatial discriminations generally. In the present case the center of the available results relates to spatial integration over various line lengths, orientations, and number of lines, but neither experiments with temporally varying stimuli nor with varying levels of brightness-produced levels of adaptation have yet been reported on the VPEL discrimination; the earlier application of conductance variation as a concept appropriate for neural modeling was carried out in a context in which the effects of adaptation level and flash durations and intensities were significant. Hopefully, the deficiency in results available regarding the elevation of VPEL will be corrected in the near future and make it possible to integrate the effects of intensity and temporal parameters into the present

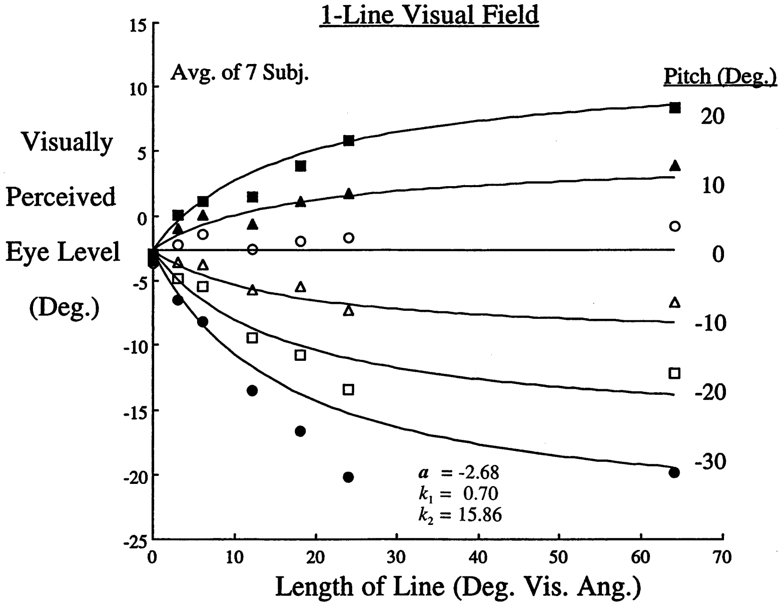

Fig. 7. Eq. (8) of the model is fitted to the results of experiments (from Matin & Li, 1994b) in which the elevation of VPEL was measured in conjunction with experimental variation of the length and orientation of the 1-line pitched-from-vertical stimulus viewed in otherwise total darkness. Average results across seven subjects over the pitch range from −30° to +20° and line lengths from 0° to 64° long are displayed (see footnote 10). The best fitting values of $\boldsymbol{a}$, k_1 and k_2 from the application of Eq. (8) were obtained for the results for each pitch separately, and then the averages of the values for the five nonzero pitches were calculated to yield a single trio of values that were employed to draw the smooth curves through all of the results in the figure. These best fitting values are −2.68° of pitch, 0.70° vis ang/deg pitch, and 15.86° vis ang, respectively.

was constrained to the median plane and the inducing lines were located at 25° to the left and/or right of the median plane. As a consequence of these experimental constraints on gaze direction and inducing line eccentricity the influence of the body-referenced mechanism can be treated as constant throughout and, as noted earlier, will enter the model as a lumped constant parameter. We include this lumped parameter as the additive constant $\boldsymbol{a}$ in the fit between model and data; the values of $\boldsymbol{a}$ that best fit the experimental results discussed below and the experimental dark VPELs are very close. Eq. (8), which contains the three constants for fitting the model to the experimental measurements, $\boldsymbol{a}$, k_1, and k_2, then yields the predicted value of VPEL:

$$\mathbf{V} = \boldsymbol{a} + \frac{k_1 \sum_{i=1}^{\boldsymbol{n}} \theta_i}{\boldsymbol{n} + (k_2/\boldsymbol{l})} \tag{8}$$

5. Fit of the model to experimental data

The first two sets of experimental results fitted to the model (Figs. 7 and 8) were obtained in experiments in which self-luminous lines were mounted on the interior pitchable wall of the otherwise completely dark pitchroom (the invisible pitchroom was employed here solely as a means or generating pitch of the lines) (Matin & Li, 1992a, 1994a,b). The first set consists of measurements of the elevation of VPEL with pitched-from-vertical 1-line stimuli of variable length and pitch. The average VPEL settings for seven subjects, each of whom was subject to all of the experimental conditions, are displayed in Fig. 7 (the results for five of those subjects were described in experiment 1 in Matin & Li, 1994b). The values for $\boldsymbol{a}$, k_1 and k_2 for the theoretical curves shown in Fig. 7 are the arithmetic averages of the best fits to each of the orientations fitted separately, and the single set of average best fit values was employed to generate all of the curves displayed.

For three of the seven subjects whose data are averaged in Fig. 7, measurements were also obtained with the parallel, 2-line, pitched-from-vertical, equal-length stimulus at four lengths and six line orientations (data originally presented in exp. 3, Matin & Li, 1994b). Fig. 8a displays the average results for these three subjects for each of the six line orientations separately in a form that permits direct comparison between the fits to both 1-line and 2-line data with the same set of constants for

---

formulation. Although some aspects of the second stage of the present model are described by reference to a single neuron, there is no intent to suggest that a single neuron can completely control the process of mediating the visual influence as may be the case in the threshold for detection. Nevertheless, the visual influence on the perception of elevation is exerted without significant variation over the entire visual field, and for a set of similar second stage neurons to produce such a uniform wide-field effect, modulation of their outputs would need to be synchronized; a common source would continue to be necessary, and this suggests that it will be unitary at some point prior to its input to stage 3.

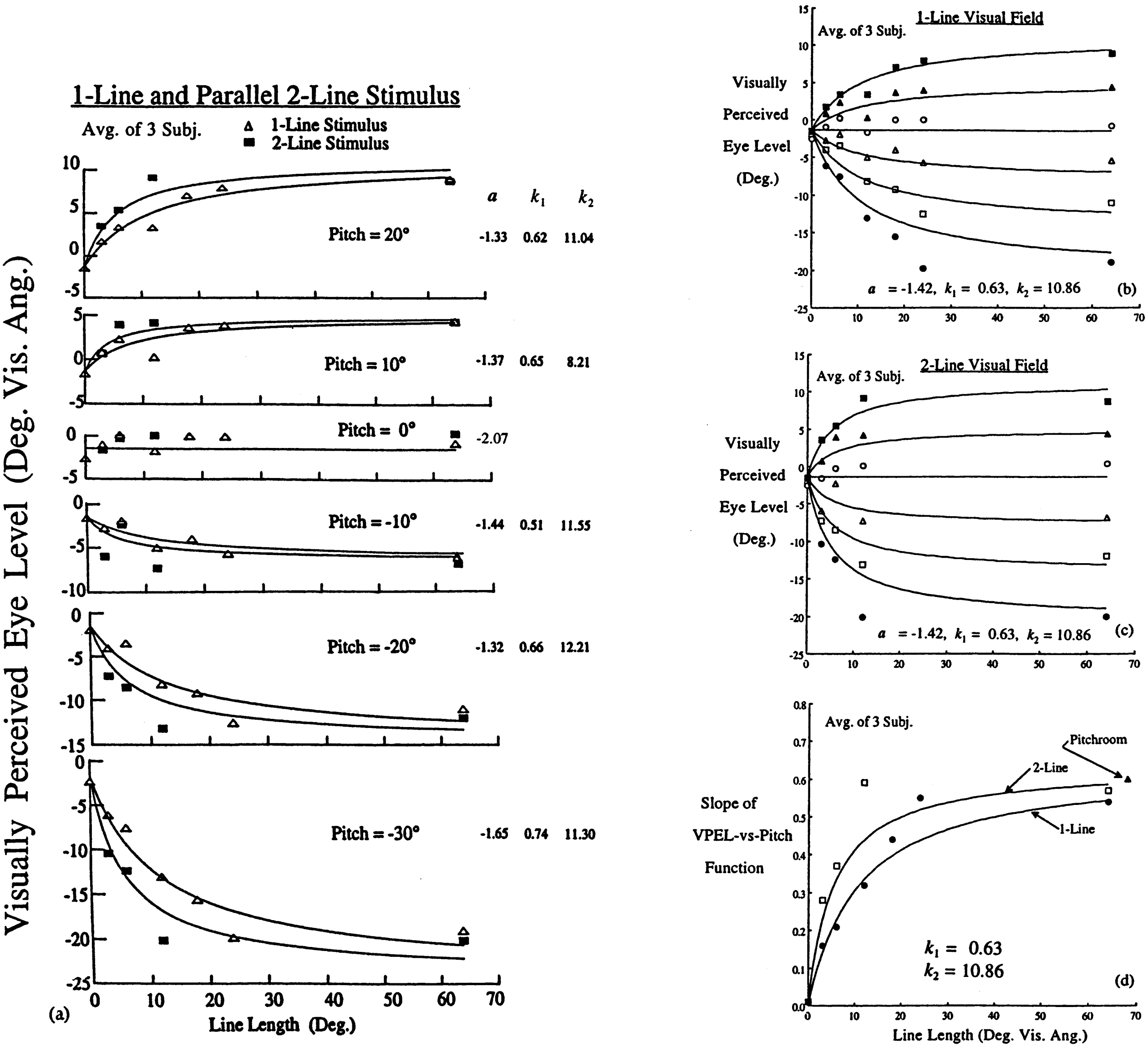

Fig. 8. Average results for three subjects viewing the 1-line and 2-line visual fields are displayed in (a) separately for each pitch. The best fitting values of $\boldsymbol{a}$, k_1 and k_2 in (a), employing Eq. (8), were determined separately at each pitch for the average of the 1-line results for the three subjects. These values were then employed to fit the 2-line results for the same pitch. Since the value predicted for V_A for zero pitch (erect) is zero for all line lengths, the predicted value at each of the line lengths at zero pitch for both the 1-line and 2-line stimuli is the average value of $\boldsymbol{a}$; thus, the single line through the results for zero pitch is drawn through the average of all 1-line and 2-line values; predicted values for k_1 and k_2 at zero pitch are indeterminate. The single set of averages across the different pitches of the best fitting values of $\boldsymbol{a}$, k_1 and k_2 in (a) are fitted to all of the 1-line results in (b) and to the 2-line results in (c). Using the same values of $\boldsymbol{a}$, k_1 and k_2 that were used in (b) and (c), in (d) we plot the curves generated by Eq. (9) to the slopes of the average VPEL-vs.-pitch functions for the 1-line (filled circles) and 2-line (open squares) results at the different line lengths for the three subjects. Also displayed in (d) is the slope of the VPEL-vs.-pitch function measured with the fully-illuminated, complexly-structured pitchroom (filled triangles) sketched in Fig. 1. As noted in the text, this value was fitted to the model in the following way: there are eight pitched-from-vertical segments that fill the horizontal extent of the front surface of the pitchroom, and since the height of the visible front surface is 64°, the slope for the full pitchroom is plotted at the abscissa value = 64°; thus, the fit employed $\theta = 64$ and $\boldsymbol{n} = 8$; with the same values of k_1 and k_2 that were used to fit the 1-line and 2-line results, the theoretical function that was obtained (not shown) passed through the data point measured for the pitchroom.

both.[10] The constants shown to the right of each panel are the best fitting values (least squares) to the 1-line data for that orientation. The two smooth curves in each panel were calculated with those constants; the curve with smaller absolute values on the ordinate in each panel is the best fit to the 1-line results; the curve with the larger absolute ordinate values employs those

---

[10] Although the original report (Matin & Li, 1994b) described results for five subjects in the 1-line experiments and three subjects in the 2-line experiment, only one of these participated in the two experiments. The two other subjects who participated in the 2-line experiment were subsequently run in the complete 1-line paradigm

same constants to fit the 2-line results ($\boldsymbol{n} = 2$). The variation in constants needed for best fit to the 1-line results at different orientations in Fig. 8a is not generally large ($-1.65 < \mathbf{a} < -1.32$; $0.62 < k_1 < 0.74$; $8.41 < k_2 < 12.21$). Fig. 8b and c display the results for the three subjects in a form that permits comparison across orientations for the 1-line results and the 2-line results separately. Thus, as in Fig. 7, a single set of constants was applied to all of the results in Fig. 8b and c; the constants were the averages of the best fits to the 1-line results alone; these values are $\boldsymbol{a} = -1.42°$, $k_1 = 0.63$ degrees of visual angle/degree of pitch, and $k_2 = 10.86$ visual angle degrees.

There are some deviations in Fig. 8 between the $\boldsymbol{n} = 2$ curve and the 2-line results which suggest that the model, while providing acceptable fits, underestimates the measured values. This is consistent with the fact that the quantitative development in the present model makes no attempt at accounting for the small increase of the influence from the bilaterally symmetric 2-line stimulus over that from a single 1-line stimulus whose length equals the sum of the lengths of the two lines contained in the 2-line stimulus (an interpretation of this fact that is consistent with the model is described as the first point in Section 8 below). Given the differences between the pools of subjects in Figs. 7 and 8, the difference in best fitting values between the fits in the two figures is not large; the value of k_1 in Fig. 7 lies within the range shown in Fig. 8; the value of k_2 in Fig. 7 for the average of seven subjects is somewhat larger than the values in Fig. 8. The dark values at each orientation were measurements made in the session devoted to that particular orientation; nevertheless, these values are all close to each other (as they were in Fig. 7) and the values of $\boldsymbol{a}$ fitted to the results at the different orientations are similarly close; the 1° difference in the value of $\boldsymbol{a}$ between Figs. 7 and 8 is not atypical for differences among dark values for different subject pools.

The slope of the VPEL-versus-pitch function has been employed as the most characteristic single measure of the visual influence in previous work on VPEL. The model's prediction for these slopes, $\mathbf{dV}/\mathrm{d}\theta$, is

$$\frac{\mathbf{dV}}{\mathrm{d}\theta} = k_1/(1 + [k_2/\boldsymbol{nl}]) \tag{9}$$

and is shown in Fig. 8d along with the slopes of the VPEL-versus-pitch functions plotted for each combination of pitch and line length for both the 1-line and 2-line results. The same single pair of values of k_1 and k_2 employed in Fig. 8b and c were used in Fig. 8d for both theoretical curves.

The third, fourth, and fifth sets of experimental results fitted to the model (Fig. 9) were obtained between 3 and 6 years later with a different experimental setup and different pool of subjects. Whereas the earlier results (Figs. 7 and 8) were obtained by mounting individual visible lines on the pitchable wall of the dark pitchroom and pitching the entire room, the later results (Fig. 9; reported in Li & Matin, 1992; Matin & Li, 1999a, 2000) were obtained by mounting each line on a separate standalone pitchable surface. An important difference between the two experimental setups was that whereas the axis for pitch of the lines on the standalone surface was at true eye level and within the surface so that the axis bisected the length of each line at all orientations, for the pitchroom the pitch axis was close to the subject (between the subject and rear wall of the pitchroom), the axis was below true eye level, more than half of the extent of each line was above true eye level when the room was erect, and as a result of this arrangement decreasing topbackward pitch and increasing topforward pitch was accompanied by an increase in the height of the lines in the visual field (see Matin & Li, 1992a, for quantitative details). This latter variation of height contributes a visual influence of 10–15% of the height change to the values of VPEL relative to values measured without the height variation as in Fig. 9[11], a contribution measured with both short (12°-long) and long (64°-long) lines (Li & Matin, 1990c; also additional unpublished experiments). The experi-

---

and these results are included in the pool of seven displayed in Fig. 7. Since we fit the average values of both sets of results with a single set of parameters from the model in Fig. 6, and since the idiosyncratic aspects of individual subjects should be represented in either both sets or neither for a common fit, the results we show in Fig. 8 are for the three subjects for whom results are available in both experiments. Since $\theta_{\mathrm{i}} = 0$ for the erect condition, the results cannot be fitted to the model; for this case, however, the average VPEL is -2.07, close to values of $\boldsymbol{a}$ in the other conditions as expected.

[11] The 10–15% measured difference in the bias due to variation in the height of the inducing lines relative to true eye level (noted above) is manifested as a difference in y-intercept (Li & Matin, 1990c). However, in the pitchroom where the height change is correlated with the change in pitch during a single series of measurements, a 10% bias generates approximately a 17% difference in the slope of the VPEL-versus-pitch function, as shown by the following calculation: Assume a 0.40 VPEL-versus-pitch slope with pitch axis at a fixed height; with variation of pitch from $-30°$ (topbackward) to $+30°$ (topforward) a 24° variation in VPEL is then generated; if an increase in height of the pitch axis generates a 10% change in y-intercept with no change in slope when the entire VPEL-versus-pitch function is measured at each of several pitch axis heights, a correlated height variation of 40° adds $-2°$ and $+2°$ to the pitch-alone-produced VPELs resulting from $-30°$ and $+30°$ pitch, respectively; this 4° addition to the 24° pitch-alone-produced variation increases the measured slope to 0.47, a 17% increase above the pitch-alone-produced slope. Similarly, a 15% bias due to height variation increases the measured slope by *25%* to a value of 0.50. The slope of the 2-line functions for the 64^{0}-long lines measured with height of the pitch axis variable were 0.52 (Matin & Li, 1992a) and 0.56 (Matin & Li, 1994a); this compares to values of 0.40 (Li & Matin, 1995a) and 0.44 (Matin & Li, 1999a) with the pitch axis fixed at eye level, and is well explained by the difference in the influence of pitch axis height in the two cases. Similar differences are present in the 1-line results with and without pitch axis height variable.

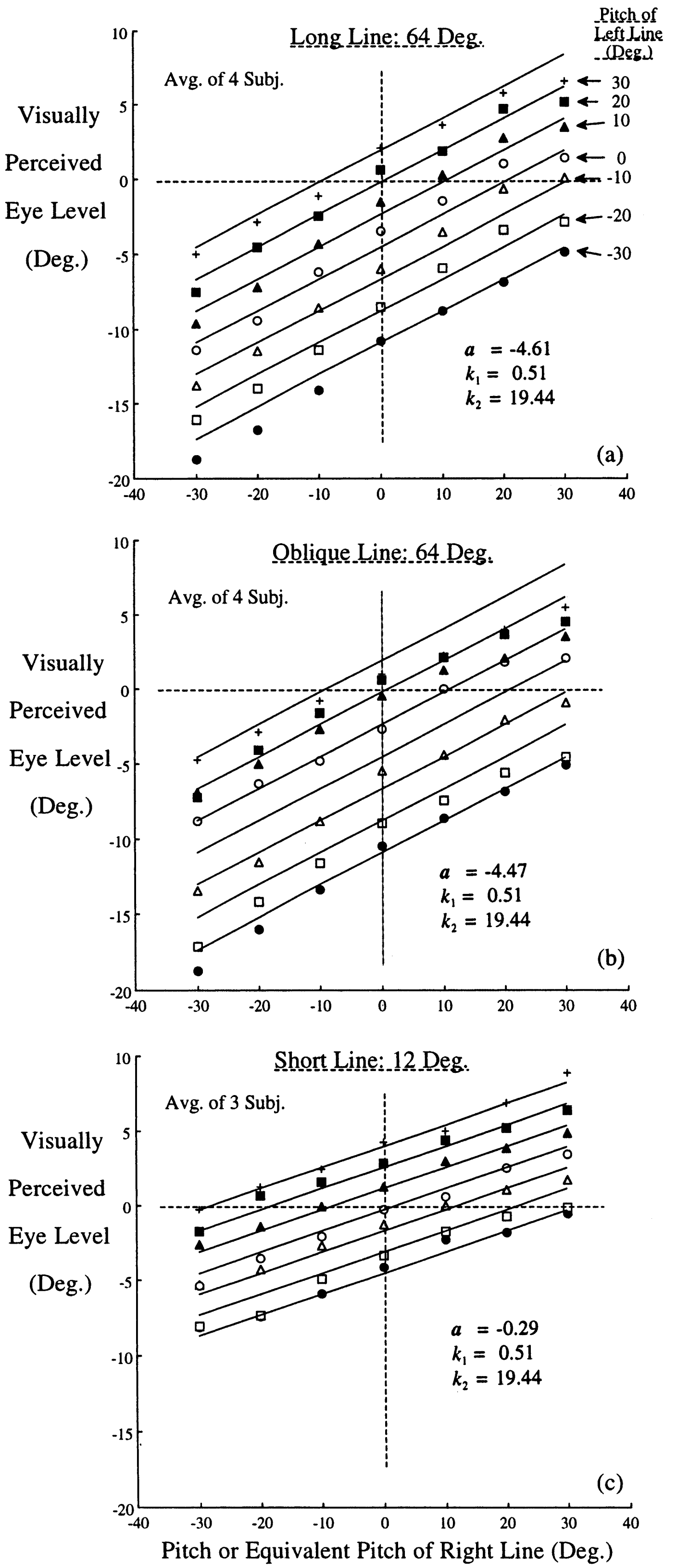

Fig. 9. Measurements of VPEL for the 2-line pitched-from-vertical visual field. Each of the two lines was set at one of seven pitches (or equivalent pitch); the average results for several subjects at all 49 combinations of orientations of the two lines are displayed. The straight lines displayed in each of the three panels are predicted values from Eq. (8), see text for derivation of values for $\boldsymbol{a}$, k_1 and k_2. (a) 64°-long pitched-from-vertical lines, average values for four subjects; (b) 64°-long oblique lines from a frontoparallel plane, each of the 49 combinations strikes the same retinal orientation as one of the combinations in (a); (c) 12°-long pitched-from-vertical lines, average values for three subjects.

ments in Fig. 9 are measurements of the elevation of VPEL with long (64°-long; Fig. 9a) or short (12°-long; Fig. 9c) pitched-from-vertical lines, or long (64°-long; Fig. 9b) oblique 2-line stimuli viewed in darkness in which the two equal-length lines were again presented to bilaterally symmetric locations; the two simultaneously-viewed lines possessed different orientations in 42 of the 49 conditions in each of the three experiments (Matin & Li, 1999a, 2000). For each experiment, each of the two simultaneously-presented, equal-length lines was presented at one of seven orientations, and measurements were made with all 49 combinations of orientations of the two lines (thus, in seven of the conditions in each case the two simultaneously-presented lines were parallel, as in Fig. 8). In each condition in Fig. 9b the oblique lines were presented within a frontoparallel plane and possessed the equivalent pitch to one of the conditions with pitched-from-vertical lines in Fig. 9a (retinal orientation in oblique and pitch conditions were matched). The results for the short-line experiment are the average values for three subjects, the results for the two long-line experiments are the average values for four subjects all of whom participated in both long-line experiments; only one of the subjects participated in all three experiments; this subject (WL), one of the authors, is the only one who also participated in the two experiments of Fig. 8a and b. The results of both experiments can be used together to obtain a fit to the model in a way that is free from any bias due to height variation of the pitch axis: Using Eq. (8) with $\boldsymbol{l}$ and $\boldsymbol{n}$ fixed (as in Fig. 9), we can write $\mathbf{V}-\mathrm{c}=d\Sigma\theta_{\mathrm{i}}$ with c and d as constants. The best-fitting values of d to the results in Fig. 9a and c are 0.22 and 0.14, respectively. Since $d=k_1/[\boldsymbol{n}+(k_2/\boldsymbol{l})]$ is a linear equation in the two unknowns, k_1 and k_2, by employing the results in Figs. 9a and 9c simultaneously (long and short pitched-from-vertical lines, respectively), the two linear equations can be solved for k_1 and k_2: thus, employing the best-fitting values of d, $k_1=0.51$, and $k_2=19.44$. For the long oblique lines in Fig. 9b the best-fitting value of $d=0.21$, and along with the short line results in Fig. 9c (no other short line results exist) similar calculations yield $k_1=0.47$, and $k_2=16.70$. Employing these values of k_1 and k_2 the best-fitting values of $\boldsymbol{a}$ are obtained as -4.61, -4.47, and -0.29 for the long pitched-from-vertical, oblique, and short pitched-from-vertical lines in Fig. 9a, b, and c, respectively.[12] These fitted values of $\boldsymbol{a}$ in Fig. 9 are within 4° of those in Figs. 7 and 8, and are within the range spanned by the values determined in a number of other experiments for the intercept of the VPEL-versus-pitch function (and the dark VPEL as well). However, the values of k_1 are smaller and the values of k_2 are larger in the experiments with the pitchable surface (Fig. 9) than those in the pitchroom (Figs. 7 and 8). These differences are largely a consequence of the differences in location of the pitch axis in the two cases and the resultant differences in the way in which stimulus height varies as part of the variation in pitch[13]; some additional (unknown) contribution is also made by the differences in subject pool.

The theoretical fits in Fig. 9 are very good overall, with those for the short, 12°-long lines containing only small deviations and showing no signs of any systematic deviations from the data; deviations of data from theory for the 12°-long lines in Fig. 9c are no more than would be expected from normal experimental variability. Those for the 64°-long lines in Fig. 9a, however, while good also, contain some systematic deviations for the cases in which both lines possess topforward pitch. Although both sets of theoretical curves are linear and each set consists of equidistant parallel lines, the results for the short lines in Fig. 9c conform to a process of linear summation between the influences of the two lines whereas the results for the long lines are a consequence of nearaveraging between the influences of the two constituent lines: This difference, noted earlier (see discussion related to Eq. (1)), is indicated by a slope of

---

[12] With both $\Sigma\theta_{\mathrm{i}}$ and $\boldsymbol{l}$ as experimental variables in the experiments of Figs. 7 and 8, it was possible to fit the three constants, $\boldsymbol{a}$, k_1, and k_2 (as was done above). However, when $\boldsymbol{n}$ and $\boldsymbol{l}$ are set at fixed values, as in each experiment in Fig. 9, k_1 and k_2 lose their independence as a result of the linear relation, $d=k_1/(\boldsymbol{n}+k_2/\boldsymbol{l})$, between them; in effect, only d [and c] is fitted to a linear function of the experimental variable $\Sigma\theta_{\mathrm{i}}$, and once d is determined by the fitting process, if k_2 is assumed to possess a particular value, a particular value of k_1 results, and if k_2 is assumed to possess a different value, the best-fit value of k_1 also changes in a way as to fit the linear relation. In order to gain some additional perspective on the relation between model and data, we took a different approach; we employed the average value of k_2 determined from the experiments in Fig. 8, 10.86, and obtained values of 0.48 and 0.45 for k_1 for the long-line and short-line results in Fig. 9, respectively. The closeness of these values to the value of 0.51 resulting from the different fitting process described in the text suggests some robustness to the values obtained. We also call attention to the fact that, even with the additional degree of experimental freedom in the experiments carried out in the pitchroom, the fits shown in Figs. 7 and 8 were not accomplished with θ_{i} and length varied simultaneously during the fitting process (the fitting was done with *ASYSTANT+* [1986]). Instead, each of those fits in Figs. 7 and 8a was carried out separately with each fixed value of θ_{i} with only $\boldsymbol{l}$ treated as an experimental variable. The fits to the three constants could be (and were) accomplished in Figs. 7 and 8a because the relation fitted with $\Sigma\theta_{\mathrm{i}}$ fixed was a nonlinear function of the experimental variable, $\boldsymbol{l}$, that does not reduce to a two-constant form.

[13] The variation in height in the field of the visual stimulus with change in orientation in the pitchroom can be treated as a simple combination of rotation around a fixed-height pitch axis in the rear wall of the pitchroom on which the line stimuli are mounted in combination with a translation of the axis of pitch that was systematic with pitchroom orientation, and so the inducing stimulus of the lines-in-darkness in the pitchroom can be treated as equal to an additive combination of the stimulus on the pitchable surface plus a translation of pitch axis). We have described things in this way previously (Li, et al., 2001). However, it is important to call attention to the fact that such a resolution into a combination of rotation + translation, while convenient for many purposes, is arbitrary.

0.99 (slope required for perfect linear summation = 1.00) across all 49 short-line conditions between the 2-line VPEL and the additive sum of the two 1-line VPELs for the two constituent lines (Matin & Li, 2000), whereas the comparable slope for the 49 conditions in the long-line case is 0.61 (slope required for averaging = 0.5) (Matin & Li, 1999a). The oblique long-line data in Fig. 9b appear more variable than that for the pitched-from-vertical lines in Fig. 9a and the fits contain more by way of systematic deviations; nearaveraging held for these results also with the slope of the relation between the 2-line VPEL and the additive sum of the two 1-line VPELs for the two constituent lines equal to 0.58. We return to the systematic deviations in Fig. 9a and b in point 2 in Section 8 (see also Fig. 11).

Up to this point, all of the measurements fitted to the model in the present section have been with 1-line or 2-line pitched-from-vertical or roll-tilted stimuli viewed in otherwise complete darkness. We now extend the use of the model to the well-illuminated, complexly-structured pitchroom. Rewriting Eq. (8), we have

$$\mathbf{V} = \boldsymbol{a} + \frac{\boldsymbol{l}k_1 \sum_{i=1}^{\boldsymbol{n}} \theta_i}{\boldsymbol{nl} + k_2} \tag{10}$$

and since we are dealing with a single rectangular, pitched-only surface at an angle θ, then $\theta_1 = \theta_2 = \cdots \theta_{\boldsymbol{n}} = \theta$, and so $\Sigma_i^n \theta_i = \boldsymbol{n}\theta$, and with $\boldsymbol{nl} > \uparrow > k_2$, we have

$$\mathbf{V} \approx \boldsymbol{a} + k_1\theta \tag{11}$$

In the original report of work with the illuminated pitchroom (Matin & Fox, 1986, 1989), it was proposed that

$$\mathbf{V} = k_{\mathrm{v}}\boldsymbol{V} + k_{\mathrm{b}}\boldsymbol{B} \tag{12}$$

where the contributions of the body-referenced mechanism and the visual influence were set equal to $\boldsymbol{B}$ and $\boldsymbol{V}$, respectively, and k_{b} and k_{v} were weighting constants for which $k_{\mathrm{b}} + k_{\mathrm{v}} = 1$. In the present report the contribution of the body-referenced mechanism was set equal to $\boldsymbol{a}$, and if we equate $\boldsymbol{a}$ to $k_{\mathrm{b}}\boldsymbol{B}$, and set $\boldsymbol{V} = \theta$ as was done in the original report, Eq. (11) becomes:

$$\mathbf{V} = k_1\boldsymbol{V} + k_{\mathrm{b}}\boldsymbol{B} \tag{13}$$

Thus, if we can show that k_1 (the theoretical value in the present model that is based on the assumption that the total visual influence equals a value that is a linear combination of the separate influences of individual oriented lines) is close to k_{v}, (the theoretical value of the total visual influence of the pitchroom from the earlier model), then we have a significant basis for believing that the two formulations represented by Eqs. 10 and 12, refer to the same mechanism. In an experiment in which eight subjects set VPEL while viewing the illuminated pitchroom (Matin & Li, 1992a), the average value of k_{v} was equal to 0.63. Five of those subjects were also part of the group of seven involved in the 1-line experiment whose results are plotted in Fig. 7; for those five the calculated value of k_1 equals 0.68. The original formulation assumed that VPEL was determined by a weighted average of the body-referenced mechanism and the visual influence; the present model assumes that the variation in experiments under consideration is a consequence of some particular properties regarding orientation sensitivity of the neural system mediating the visual influence on VPEL (along with the contribution of the body-referenced mechanism). These are different theoretical starting points and deal with different aspects of the experimental material. The closeness of the values of k_1 and k_{v} derived from data for the same subjects points to considerable consistency in the two theoretical approaches and supports the view that both treatments do refer to the same mechanism.

In Fig. 8d the value plotted as the rightmost point is the VPEL-versus-pitch slope for the full pitchroom. This value for the full pitchroom was fitted to the model in the following way: The walls of the pitchroom are papered with a red brick design (Fig. 1a). Although the verticals between adjacent bricks on the front surface do not constitute long continuous lines, together with the continuous vertical edges bounding the front surface they present approximately 512° of visual angle extending vertically when the pitchroom is erect. This 512° is made up of 8 pitched-from-vertical sets of pitched-from-vertical segments that fill the horizontal extent of the front surface of the pitchroom, and since the height of the visible front surface is 64°, we treat this surface as the approximate equivalent of eight 64°-long lines: the slope for the full pitchroom is plotted at the abscissa value = 64°. Thus, for present purposes the fit of the result for the well-illuminated, fully structured pitchroom by the present model employed $\theta = 64°$ and $\boldsymbol{n} = 8$; with the same values of k_1 and k_2 that were used to fit the 1-line and 2-line results, the theoretical function that was obtained by the fitting process (not shown) passes through the data point measured (and plotted) for the pitchroom. The consistency between the two theoretical treatments implies that the present model applies to complexly structured, well illuminated visual environments as well as to the dimly illuminated 1-line and 2-line visual fields for which it was originally derived.

6. Some relations to neuroanatomy

Although the three stages of the neurophysiologically-based model are employed to describe the main features of the results of psychophysical experiments, additional work will be needed to enhance contact with the underlying neuroanatomy. This section indicates some considerations regarding the neuroanatomy relevant to the building of useful bridges across the psychophysical/neuroanatomical gap.

The growth of the VPEL response with line length extends to lengths of at least 20° and goes on to an asymptote at 60° or more (Figs. 7 and 8), exceeding considerably the classical 1°–3° lengths in cat and monkey (Hubel & Wiesel, 1962, 1974, 1977) of individual orientation-sensitive receptive fields in V1. Later work has disclosed the existence of pyramidal cells in layer 6 of V1 for which the response to oriented bars grows through at least 16° (Gilbert, 1977) and of long-ranging axons of complex cells making periodic clus-tered excitatory horizontal connections with units in columns of similar orientation sensitivity within adjacent hypercolumns (Gilbert & Wiesel, 1983; Ts'o, Gilbert, & Wiesel, 1986), findings that are consistent with the view that the individual neurons providing output from stage 1 of the present model reside in V1 (with caveats regarding species differences between man, monkey, and cat applying here and below). A much larger range of lengths of oriented receptive fields are found in neural units in V6 along with several other properties that would be expected from an area that mediated stage 2 and/or stage 3 processing of the present model (Galletti, Battaglini, & Fattori, 1991). The results we model and the model itself not only requires summation along the length of an individual line, but similar magnitudes of summation between line segments in different hemispheres. Two routes (not mutually exclusive) through which this may occur are indicated: (a) Some receptive fields in occipital cortex straddle the midline and receive inputs from both hemispheres, and at least some of these travel via the corpus callosum (Berlucchi & Rizzolatti, 1968; Hubel & Wiesel, 1967; Hubel, 1988; Zeki, 1993). As one moves from lower-numbered to higher numbered visual areas in occipital cortex (from V1 to V6)[14] callosal connections between bilaterally symmetric projections in the two hemispheres between either same or 'successive' visual areas extend further from the representation of the vertical meridian to regions serving more peripheral retinal eccentricities and become more diffuse (Zeki, 1993). If stage 2 integration is mediated in occipital cortex and involves callosal connections along with subcortical connections from V1, the most likely area appears to be V6 where the callosal connections extend sufficiently far from the representation of the central vertical meridian to be effective in the present case. There is considerable traffic downward (as well as upward) from occipital cortex to a number of subcortical regions in monkey and cat, particularly from layers 5 and 6. These regions include superior colliculus, claustrum, lateral geniculate nucleus, and pulvinar (Lund, Lund, Hendrickson, Bunt, & Fuchs, 1975; Lund & Boothe, 1975; Gilbert & Kelly, 1975; LeVay & Sherk, 1981a,b; Sherk & LeVay, 1981, 1983; McCourt, Boyapati, & Henry, 1986). Although these regions are known to be linked with space perception, the functions served by the cortico-subcortical connections are not yet clear. In conjunction with callosal connections and/or separately, some of these regions may be involved in the route by which summation occurs between straight line inputs to the two hemispheres. Callaway's (1998) class IIA cells in the middle of layer 6 in V1 project to the white matter and probably to the claustrum; these appear of particular interest in the present context. (b) The inferior lobule of posterior parietal cortex is a likely location for stage 3 of the present model where the total visual influence of the oriented line stimuli is combined with the influence from the body-referenced mechanism: It is also possible that the outputs of the four groups of neural units in stage 1 of the model travel separately to parietal cortex and thus that stage 2 is localized there as well. if so, however, the path is likely to lead through regions in extrastriate cortex (see Andersen, 1987, 1989 for several such routes), and the groups would acquire their identity there. Substantial callosal connections do exist in 7a (Andersen, et al., 1985) and the receptive fields of these cells are bilateral (Andersen & Mountcastle, 1983), presumably mediated by callosal connections.

Selective responses in the inferior lobule of the right parietal cortex (Brodmann area 40) and in the left parietal cortex (precuneus region in Brodmann area 7) have been measured with fMRI in monocularly-viewing human observers viewing bilaterally symmetric oblique 2-line stimuli on a frontoparallel plane in an otherwise completely dark field, although no such response was measured to parallel arrangements of the same two oblique lines (Matin, Li, Hudson, & Hirsch, 2001). These are the stimuli that, as described above (e.g., Fig. 9c), respectively generate systematic influences on VPEL and no influences on VPEL at all. The results are consistent with the view that the posterior parietal cortex is the site for the stage 3 response of the present model for VPEL, although whether the responses are at the input to stage 3 (in which case they would reflect the output from stage 2) or the output from stage 3 (in which case they are likely to be employed to provide signals to other centers in posterior parietal cortex and/or to prefrontal cortex) was not determined.

7. Interactions between the body-referenced mechanism and horizontal line eccentricity

In describing the above model and its fit to a body of experimental data we have been at pains to make it clear that our introduction of the additive constant ***a*** and its interpretation as the influence of the body-referenced mechanism is a consequence of the fact that the experi-

---

[14] V6 lies in the anterior bank of the parieto-occipital sulcus. It appears to have been designated as V6 by Zeki (1986) and to coincide with part of an area labeled PO by Colby, Gattass, Olson, and Gross (1988). It has been referred to both as part of parietal cortex and occipital cortex.

ments were carried out with the direction of gaze constrained to the median plane and the inducing lines constrained to two bilaterally symmetric locations 25° on either side of the median plane. This treatment of the body-referenced mechanism as an additive constant has been successfully applied to VPEL in some of our previous reports where similar experimental constraints were in force (Matin & Fox, 1989). The reasonableness of this approach is indicated by the following: subjects make highly reliable but idiosyncratic VPEL settings in total darkness (Matin & Fox, 1986, 1989; Stoper & Cohen, 1989; Matin & Li, 1994a,b); dark VPELs for different individuals may be as large as 6.0° below TEL or about 4° above with an average across subjects that has tended to lie 2° to 4° below TEL. For a given subject, standard deviations of the dark VPEL across successive trials typically average about 1.0°, only slightly greater than the 0.8° that typifies VPEL settings in the presence of a visual field, although session-to-session variability is greater. Thus, the action of the body-referenced mechanism is shown by the ability of subjects to make fairly accurate and reliable VPEL settings when operating without the presence of the visual field. In addition, the y-intercept of the VPEL-versus-pitch function across individual observers is highly correlated with the dark VPEL: thus, individuals with more negative y-intercepts also manifest dark values that are more negative than individuals whose y-intercepts are less negative (Matin & Fox, 1989; Matin & Li, 1994a; Li et al., 2001); this relation is also retained across individuals when measurements are made on observers in rolled-to-horizontal as well as erect postures although there is a significant difference in the values between the two postures (Li et al., 2001). This relation between dark value and y-intercept adds to the support of the use of the additive constant as a representation of the influence of the body-referenced mechanism. Since the VPEL-versus-pitch function is nearlinear, specifying it as an additive combination of the y-intercept and scaled pitch provides a very close representation of the function itself.

However, when variation of gaze direction is permitted, the body-referenced mechanism can no longer be treated as a fixed constant; it's significant contributions and the complexity of its contribution become manifest (see Li & Matin, 1991a, 1993; Dallal et al., 1993; Li et al., 2001; Chelette et al., 1995; Matin & Li, 1995a; DiZio et al., 1997). These contributions are particularly clear in three experimental contexts: (a) when viewing a stationary line the retinal image location of the line changes in correspondence with the observer's direction of gaze. If the induction-by-lines of the VPEL setting simply depended on the location of the retinal image, systematic changes of gaze should then produce significant, systematic changes in VPEL that are identical to those that do occur when the same retinal image location results from change in eccentricity of the physical line stimulus with the eye constrained to the median plane (Li & Matin, 1990c, 1991a, 1993; Matin & Li, 1995a). However, neither changes in the orientation of the eye in a stationary head nor changes in orientation of the head on the neck have yet resulted in any significant change in the VPEL setting for the erect observer in the presence of a stationary pitched-from-vertical 1-line or 2-line stimulus, or the fully illuminated, well-structured pitchroom. Such an approximation to perceptual stability in the face of changes in eye and/or head orientation implies that the VPEL setting make use of head-centered information about eye position and body-centered information about the head-and-eyes in addition to information from the visual field regarding visual orientation. The signals regarding head and eye position are significant contributors to stabilizing against mislocalization (Li & Matin, 1991a, 1993; Matin & Li, 1995a). (b) In an earlier set of experiments with subjects for whom the signals to extraocular muscle had been experimentally weakened by the use of curare, the resulting large mislocalizations of VPEL produced in darkness were shown to be dose-dependent (and hence systematic with the amount of muscle weakening) and dependent on the vertical orientation of the eye in the orbit, although not dependent on head orientation relative to the body. The paresis-produced mismatch between the extraretinal signal regarding eye position and actual eye position provided the basis for the perceptual mislocalization (Matin et al., 1982; Matin, Stevens, & Picoult 1983). (c) A separate basis for the assumption of extraretinal processes derives from work with spatial localization during saccadic eye movements where, in experiments involving single point targets in darkness, cancellation models that assume that localization is based on the additive combination of retinal and extraretinal signals in the face of saccadic eye movements, are required to account for some aspects of mechanism (Matin, 1972, 1982, 1986; Li & Matin, 1990a,b, 1997a).

But the complexity involved in dealing with the body-referenced mechanism is not simply a question of separating the various components of the mechanism and dealing with each and with their combination. Significant interactions occur between some of the components of the body-referenced mechanism and some parameters of the visual influence. A significant segment of the problem of dealing with the body-referenced mechanism theoretically is a consequence of the way in which inducing line eccentricity interacts with the extraretinal signal for eye position. We will indicate the resulting complication by a single example: The change in retinal location of a point target is identical in the following two instances: (a) a foveated target is horizontally displaced by some amount, X°, while the subject's direction of gaze is unchanged; (b) the subject's direction of gaze is horizontally displaced by X° in the opposite direction to that in (a) while the target's physical direction is unchanged. Although many issues remain, a relatively simple treat-

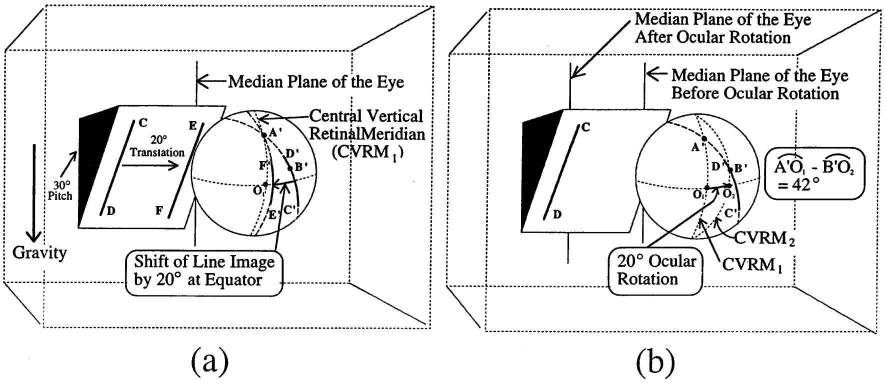

Fig. 10. This figure displays the different consequences for the retinal image that results from a displacement of a pitched-from-vertical line on a pitched-only plane, and a shift of the direction of gaze by the same angular amount. The sphere is an approximation to an eye that is stationary in (a) but rotates with change of gaze in (b). The coordinates of each figure are fixed in physical space (the space of the page.); the view on the page is from behind the eye. In (a) line CD, located on the 30°-pitched-only plane at a horizontal eccentricity 25° to the left of the median plane of the stationary eye, is translated rightward by 20° to EF, 5° to the left of the median plane. $CVRM_1$ represents the central vertical retinal meridian in the median plane of the eye; O_1 represents the fovea lying on the equator. Point A′ is a common intersection point on $CVRM_1$ for great circles containing the images of all pitched-from-vertical lines on the 30°-pitched-only plane. In (b) the eye rotates 20° leftward so that the fovea is shifted from O_1 to O_2 on the eye's equator and the location of the central vertical retinal meridian is rotated by 20° in physical space from $CVRM_1$ to $CVRM_2$. CD and its retinal image C′D′ remain in the same physical locations as in (a). Thus, the intersection of the center of the line's image (intersecting the equator at eye level) strikes the same retinal point in (b) as it did following the stimulus movement in (a), 5° to the right of the fovea. But the line image's great circle intersects the new orientation of the CVRM, $CVRM_2$, at B′ instead of at A′, a shift on the retina by 42° (i.e. $A'O_1 - B'O_2 = 42°$); this is an indication of the large difference in retinal orientation of the image of the line resulting from rotation of the eye in a stationary visual field [as in (b)] as compared to that resulting from a shift of the line with a stationary eye [as in (a)].

ment that incorporates an extraretinal signal regarding eye position is sufficient to model some aspects of the influences on perception for this case ('cancellation model'; Matin, 1972, 1982, 1986; Li & Matin, 1990a,b, 1997a).

However, the analogous identity in the change of retinal position does not hold if the visual stimulus is a line. We describe the significant difference between the change in retinal stimulation that results from a displacement of a line and rotation of the eye by way of the example in Fig. 10 where we treat the sphere as an approximation to an eye that is stationary in (a) but rotates with change of gaze in (b): The 3-dimensional box containing the stimulus surface and the eye is fixed in physical space. The two great circle coordinates employed below are: location on the central vertical retinal meridian, and location on the equator; these two coordinates are fixed on the sphere representing the eye:

(a) In Fig. 10a suppose that, with gaze fixed in the median plane of the eye at eye level (O_1 is the fovea), a pitched-from-vertical line (CD) on a 30°-topforward pitched-only plane is located at a horizontal eccentricity of 25° to the left of the eye's median plane and is centered at eye level. The great circle coordinates of its image, C′D′, defined by intersection of the great circle containing the image with $CVRM_1$, and with the equator are thus A′ (60° above the equator), and a point 25° to the right of the fovea. These two coordinates define the *retinal* orientation of C′D′. If CD is translated rightward by 20° to EF, to be centered 5° to the left of the median plane of the stationary eye, the great circle coordinate of C′D′ on $CVRM_1$ remains at A′ and the great circle coordinate on the equator shifts to a point 5° to the right of the fovea; these two points define the retinal orientation of E′F′.

(b) But if the front of the eye rotates to the left by 20° (Fig. 10b) and line CD remains stationary, the line's image remains fixed at C′D′ in physical space whereas the orientation of the CVRM in physical space undergoes a rotation by 20° from $CVRM_1$ to $CVRM_2$. Thus, the center of CD's image (intersecting the equator at eye level) strikes the same retinal point as it did following the stimulus movement in Fig. 10a, 5° to the right of the fovea. But the line image's great circle, now intersects $CVRM_2$ at B′ instead of at A′, a shift on the retina by 42° (i.e. $A'O_1 - B'O_2 = 42°$).

Thus, a 20° horizontal eye movement shifts the horizontal location of a fixation point by 20° on the retina, putting the point on the same retinal location that a 20° displacement of the point in the stimulus world would if gaze were fixed; but the analogous identity does not hold for any of the other points on the line; in the example in Fig. 10, we show this failure by the change in orientation of the image of the pitched-from-vertical line relative to the retina—the 42° shift of the intersection of the line's great circle with the CVRM from A′ to B′. The 1:1 correspondence between the magnitudes of ocular rotation and retinal shift of the fixation point (or of any other target at eye level) has underlain the use of the cancellation mechanism as a model for treatment of perceptual stability in the presence of eye movements. However, the 42° differential in a retinal coordinate in the example indicates that it does not apply unmodifed generally to line stimuli, and by extension, to complex visual fields. Although we have described matters by employing a projection sphere with a great circle coordinate system, the point we make is essentially coordinate-free. It results from the difference between the consequences of a translation (in the stimulus domain) and rotation (of the eye). Our reason for choosing to describe the shift of a point relative to the CVRM (A′ to B′) within a great circle coordinate system for our example lies in the fact that our emphasis here is on visually pitched stimuli, and points on the CVRM such as A′ are invariant points for all pitched-from-vertical lines on a frontoparallel plane that are pitched at a given orientation.[15]

The differential impact on retinal orientation of line displacement and eye movement depends on several parameters related to stimulus line location and orientation. These considerations have a major impact on the required experimental material and the modeling needed to deal with changes in gaze direction and the employment of extraretinal eye position signals when the interest is in the consequences for line stimuli. Enough of the appropriate experimental material that is required to deal with these matters is not yet available. Following the completion of some further experiments with VPEL involving systematic variation of several components of the body-referenced mechanism (several with point targets have been noted above) (Li and Matin, 1990c, 1991b, 1993, 2001a; Matin and Li, 1995a), they will be dealt with in a subsequent article where the constant, $\boldsymbol{a}$, representing the body-referenced mechanism will be broken out in a more general and more complex theoretical development than we present here.

8. Further considerations

The fits of the model to the results in Figs. 7–9 and the consistency of the present model with the earlier formulation (Matin & Fox, 1989, 1990) are promising. The discussion in this section will separate several aspects of the relation between data and the model that require further attention, attempt to provide additional perspective on them, and point to some directions where future research is needed:

1. Although the linear summation measured between two short bilaterally symmetric lines of all combinations of orientations (Matin & Li, 2000) is well-treated by the present model, there is a small increase in the amount of summation between two short bilaterally symmetric parallel lines over the magnitude of summation between two segments of a coextensive line of the same total length (Matin & Li, 1994b). The model as described above does not provide for this increase, and some of the deviations between model and data for $\boldsymbol{n} = 2$ in Fig. 8 are a consequence of this. Although it is possible that the increased effect from two short bilaterally symmetric lines is a consequence of some increase in summation for bilaterally symmetric components over summation among ipsilateral components, we have no evidence for or against such a difference. However, we do have good support from our previous experiments for the following interpretation based in part on the operation of Sherringtonian (1929) occlusion: Whereas the two short lines of the bilaterally symmetric two-line stimulus stimulate entirely separate sets of orientation-selective units in V1 (since the separation is between the two hemispheres), the single short line of double length stimulates neural units with overlapping V1 receptive fields around the region of adjacency between the two halves of the double-length single line. However, the portion of the single line at the region of adjacency may provide no useful addition over that which would be provided by one of the lines needed to generate the influence on the elevation of VPEL. In effect, two short spatially separated colinear lines may be more efficient in generating a response than one continuous line: those neural units at the end of a line which also service the adjacent dark region beyond the line's end may receive sufficient stimulation so that they can contribute to the total response to the line. If this is the case, then a continuous line would be expected to generate less total response than if the line were to be cut at its midpoint and its two pieces were separated. This interpretation receives strong support from experiments with two bilaterally symmetric, simultaneously-viewed, linear, 64°-long point arrays containing equally separated 18 minarc points (Li & Matin, 1992): The experiments examined 63 different combinations of pitch and numbers of points in the linear arrays. The slope of the VPEL-versus-pitch function increased along a negatively accelerated function with the number of points in a linear array, reaching a slope for 25 points that equalled the slope measured with the continuous line stimulus (slopes of 0.32 vs. 0.33). But, with only 25 points within each 64°-long array, the centers of adjacent points were separated by 2.5°, and this leads us to infer that most of the visual stimulation in the continuous line is not needed in order to obtain the influence on the elevation of VPEL; these results with point targets thus support the above interpretation of the increase in the influence produced by two spatially separated lines over the influence by a single line of the same total length.

2. The separation of influences into the numerator for the magnitude of pitch (or equivalent pitch) and into the denominator for line length in Eq. (7) is likely to be too simple, a simplicity that goes back to the assumptions underlying the loop equations of Eq. (2).

---

[15] Obviously, the problem we point to above does not exist if the eye were to rotate in a spherical stimulus field centered at the nodal point of the eye. However, following such considerations at this point is of no particular use here.

These equations contain the model's assumptions about the basics of the nervous system underlying the second stage of the model: The assumption that the change in conductance is proportional to the length of a line is similar to assuming that all first stage neural units in V1 which serve a single line have receptive fields of the same length. The assumption that the second stage receives inputs from all of these V1 units but that ***n*** is a count of lines makes it clear that combinations of neural units within a line and combinations between lines are not lumped with total disregard for membership of a unit in the response to a given line; the model employs a separate dendrite for the organization within a line, but the net current from a dendrite (each branch in the circuit of Fig. 6c) is the sum of the contributions from the separate V1 units that impinge on that dendrite whereas currents from all dendrites combine to drive the same axonal membrane. These assumptions were made without regard to the finer structure of the neural connections. Very little about the potential for organization in the thousands of spines and synaptic contacts that lie on both soma and dendrites of neurons was taken into account, nor were any considerations regarding the specifics of individual ion channels at either a synapse or axonal membrane or of the different types of neurons. Our lack of specific knowledge about its neuroanatomy—about the way in which influences among individual spines and synaptic contacts are organized—suggests that any more specific assumptions about magnitudes of impedance and voltages in the circuitry would be gratuitous. The simplicity of the loop equations is an attempt at representing the integrating neuron in its most simplest and most general form. A most likely place where further complexity might be required in the model is in the assumption of a simple proportionality between conductance and line length. The neural model employs separate degrees of freedom for postsynaptic conductance and voltage (EPSP) changes whereas the classical Hodgkin–Huxley equations link them. Although it is clear that conductance change and EPSP are linked, the classical equations fail to describe a number of properties of the electrical events even at axonal membrane generally, and events at postsynaptic membrane differ at different varieties of synapses and appear to be considerably less well characterized by the classical equations generally (Johnston & Wu, 1995); further developments, including those at the level of individual ionic channels and considerations regarding the manifold possibilities that exist regarding segregation and organization of function among spines are suggestive, particularly those that can arise from variable relations between conductance and potential change on spines (Johnston & Wu, 1995), but do not yet provide representations of the linkage whose use here significantly improves the approach we have taken. Evidence of active ion channels (Yuste & Tank, 1996; Johnston, Magee, Colbert, & Christie, 1996; Mainen & Sejnowski, 1998) complicates matters further. Surely, though, as we learn more, modeling will be able to be carried to more microscopic levels and some linkage between conductance change and potential change will be appropriate in a further development of the present model. Our choice of providing separate degrees of freedom for changes in conductance and potential frees our model from the specific form of linkage in the classical equations and permits employment of an orthogonal 1:1 mapping of them on to the two dimensions of line length and line orientation, respectively. Here we have taken advantage of this freedom in a relatively simple way. Although the growth of the influence of line length for different line orientations involves small differences in space constants (Matin & Li, 1994b), we have treated the change in unit conductance per length of stimulus line (g_S) identically for all line orientations and treated the effect of increasing orientation (θ) as a result of increasing potency or number of the synapses receiving signals for a given length of stimulus line; the latter can account for the systematic influence of line orientation on the elevation of VPEL at any line length.[16]

However, there is a downside to the independence assumption within the present model: it forces the prediction for the VPEL-versus-pitch functions for the two-line combinations in Fig. 9 to be parallel and equidistant: But there are small systematic deviations between theory and the data for the 64°-long pitched-from-vertical lines in Fig. 9a which can be represented as a convergence toward the right on the graph of the data sets for differently oriented left stimulus lines along with some decrease in the separation between successive data sets as one moves up the ordinate. The existence of the convergence and separation decrease in Fig. 9a is manifested by the small systematic decrease in the slope of the line which best fits a set of results for a constant left line pitch along with a corresponding decrease in the range of VPEL values with increasing topforward pitch (Matin & Li, 1999a, Table 1: average slope drops systematically from 0.25 to 0.20; VPEL range decreases systematically from 13.9° to 11.6°). This pattern is repeated in Fig. 9b where the results for

---

[16] Although our knowledge about the organization of fine structure of different inputs onto cortical dendrites is minimal, reasonable assumptions could be made that would allow us to construct the orientation-sensitive stimulus/response function in the first stage of Fig. 6a from a distributed set of individual V1 units with narrower tuning functions, for example, by assuming that line orientations producing larger influences on VPEL lie closer to the soma of the stage 2 neural units. Although of considerable importance any such further development of the model goes beyond what is needed here to deal with the psychophysical data under consideration; additional psychophysical experiments are required in order to allow theory to focus on these matters.

the 64°-long oblique lines of equivalent pitch are fitted to the model (Matin & Li, 1999a, Table 1: average slope drops from 0.25 to 0.19; range decreases from 14.0° to 10.6°). These deviations between data and theory indicate the need for greater complexity in the model. The form of the deviations suggests the presence of a small nonlinearity as conductance change approaches an asymptote with increasing pitch. The approach to an asymptote with length is most clear in the views afforded in Figs. 7 and 8; the suggestion of an approach to saturation with increasing pitch is most clearly reflected in Figs. 9a and 9b as both lines of the two-line stimulus become more topforward, and suggests a locus for saturation at or beyond a point of convergence for the influence of both lines, a point that would have to involve combinations of influences from both cerebral hemispheres.

The deviations between model and data in Figs. 9a and 9b may be a result of our separating changes in dendritic membrane potential and conductance and using this separation in Eq. (7). However, an alternative modification also removes a significant portion of the deviations. It involves some added complexity (as would any specific linkage between potential and conductance) and uses an additional degree of freedom to scale the topforward and topbackward channels separately and by different factors instead of assuming, as in Fig. 6, that they both scale the response to pitch or tilt by a common factor. Fits to the results in Figs. 9a and 9b are displayed in Fig. 11. The best fit of the

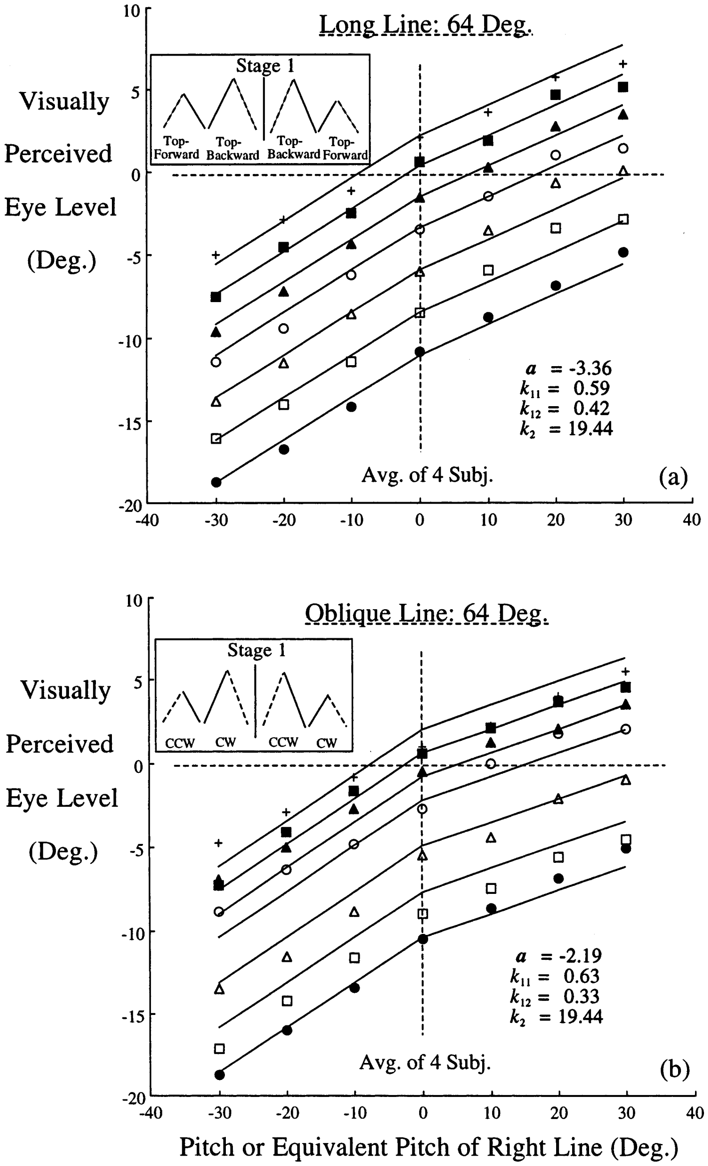

Fig. 11. The results shown in Fig. 9a for the 64°-long 2-line pitched-from-vertical visual field and the lines of equivalent pitch in Fig. 9b are fitted to a modified model in (a) and (b), respectively. In this modification the topforward and topbackward channels are permitted to scale orientation by different factors as shown in the insets.

64°-long pitched-from-vertical 2-line results of Fig. 9a to the model with this additional degree of freedom yields scales for which the response function for the topforward channel is 0.72 as large as the scale for the response function for the topbackward channel. The fit in Fig. 11a produces an appropriate convergence toward the right and some differences in separation between the functions, removing most of the deviation between theory and data. With a somewhat larger scale difference for the two channels (a scale ratio of 0.53), the modification produces considerable improvement with the oblique line results. The improvements in the fit of the model with differential scaling in Fig. 11 suggests smaller contributions to perceived elevation of topfoward pitch and its equivalent (= CCW left of median plane and CW right of median plane) that could reflect a difference in the number of neurons devoted to the different sets of orientations.

3. Individual straight lines that influence VPEL also influence the orientation of a test line that an observer has set to appear vertical within the frontoparallel plane (VPV discrimination; Matin & Li, 1991, 1992b, 1994c, 1995a, 2001). However, whereas the influence on VPEL is bilaterally symmetric as described above, the visual influence on VPV is not; instead parallel lines on opposite sides of the median plane generate the same direction of influence on VPV, and if the lines are of identical length and eccentricities on opposite sides of the median plane they generate influences of the same magnitude, whereas lines of opposite orientation on opposite sides of the median plane generate opposite influences on VPV. The significant implication here is that these combinatorial differences imply that, although the same orientation-sensitive units in V1 may provide the early cortical stage for controlling both VPEL and VPV, combinations of influence from lines on opposite sides of the median plane must involve a different neural center for VPEL and for VPV (Matin & Li, 1991, 1992b, 1994c, 1995a); specifically, the integration of the total visual influence is carried out for VPEL (Fig. 6) in a separate center from the one in which integration of the visual influence for VPV is carried out and this adds to the likelihood that these centers lie beyond V1. This is being further explored now.

Acknowledgements

Supported by grants EY 10534 from the National Eye Institute, NIH and AFOSR F49620-94-1-0397 from the Spatial Orientation Program of the US Air Force Office of Scientific Research.

References

Andersen, R. A. (1987). Inferior parietal lobule function in spatial perception and visuomotor integration. In F. Plum, V. B. Mountcastle, & S. R. Geiger, *The Handbook of Sensory Physiology. Section I: The Nervous System*. In: *Higher Functions of the Brain, Part* 2, vol. 5 (pp. 483–518). Bethesda: American Physiologcial Society.

Andersen, R. A. (1989). Visual and eye movement functions of the posterior parietal cortex. *Annual Review of Neuroscience*, *12*, 377–403.

Andersen, R. A., Asanuma, C., & Cowan, W. M. (1985). Callosal and prefrontal associational projecting cell populations in Area 7A of the macaque monkey: A study using retrogradely transported fluorescent dyes. *Journal of Comparative Neurology*, *232*, 443–455.

Andersen, R. A., & Mountcastle, V. B. (1983). The influence of the angle of gaze upon the excitability of the light-sensitive neurons of the posterior parietal cortex. *Journal of Neuroscience*, *3*, 532–548.

Asch, S. E., & Witkin, H. A. (1948). Studies in space orientation. II. Perception of the upright with displaced visual fields and with body tilted. *Journal of Experimental Psychology*, *38*, 455–477.

ASYSTANT + (1986). *Scientific software for data acquisition and analysis*. New York: Macmillan Software Company, Inc.; distributed by Keithley, Taunton, MA.

Berlucchi, G., & Rizzolatti, G. (1968). Binocularly driven neurons in visual cortex of split-chiasm cats. *Science*, *159*, 308–310.

Brandt, T., Dichgans, J., & Koenig, E. (1973). Differential effects of central versus peripheral vision on egocentric and exocentric motion perception. *Experimental Brain Research*, *16*, 476–491.

Callaway, E. M. (1998). Local circuits in primary visual cortex of the macaque monkey. *Annual Review of Neuroscience*, *21*, 47–74.

Cohen, M. M. (1973). Elevation illusion: influences of otolith organ activity and neck propioception. *Perception & Psychophysics*, *14*, 401–406.

Cohen, M. M. (1981). Visual-proprioceptive interactions. In R. D. Walk, & H. L. Pick Jr, *Intersensory perception and sensory interaction*. New York: Plenum Press.

Cohen, M. M., Ebenholtz, S. M., & Linder, B. J. (1995). Effects of optical pitch on oculomotor control and the perception of target elevation. *Perception and Psychophysics*, *57*, 433–440.

Colby, C. L., Gattass, R., Olson, C. R., & Gross, C. G. (1988). Topographical organization of cortical afferents to extrastriate visual area PO in the macaque: A dual tracer study. *Journal of Comparative Neurology*, *269*, 392–413.

Chelette, T., Li, W., Esken, R., & Matin, L. (1995). Visual perception of eye level (VPEL) under high g while viewing a pitched visual field. *Annual meeting of aerospace medical association*, p. A55.

Dallal, N., Li, W., & Matin, L. (1993). Visually perceived eye level and straight ahead: influences from visual field pitch, visual field slant, observer orientation, and gravity. *Eastern Psychological Association*, *64*, 42.

DiZio, P., Li, W., Lackner, J. R., & Matin, L. (1993). Elevation of visually perceived eye level: combined influences of gravitoinertial force level (g) and visual pitch magnitude. *Investigative Ophthalmology and Visual Science*, *34*, 778.

DiZio, P., Li, W., Lackner, J. R., & Matin, L. (1997). Combined influences of gravitoinertial force level and visual field pitch on visually perceived eye level. *Journal of Vestibular Research*, *7*, 381–392.

Eccles, J. (1957). *The physiology of nerve cells*. Baltimore, MD: Johns Hopkins Press.

Galletti, C., Battaglini, P. P., & Fattori, P. (1991). Functional properties of neurons in the anterior bank of the parieto-occipital sulcus of the Macaque monkey. *European Journal of Neuroscience*, *3*, 452–461.

Gilbert, C. D. (1977). Laminar differences in receptive field properties of cell in cat primary visual cortex. *Journal of Physiology, London*, *268*, 391–421.

Gilbert, C. D., & Kelly, J. P. (1975). The projections of cells in different layers of the cat's visual cortex. *Journal of Comparative Neurology*, *163*, 81–106.

Gilbert, C. D., & Wiesel, T. N. (1983). Clustered intrinsic connections in cat visual cortex. *Journal ofNeuroscience*, *3*, 1116–1133.

Graybiel, A. (1952). Oculogravic illusion. *Archives of Ophthalmology*, *48*, 605–615.

Held, R., Dichgans, J., & Bauer, J. (1975). Characteristics of moving visual scenes influencing spatial orientation. *Vision Research*, *15*, 357–365.

Hubel, D. H. (1988). *Eye, Brain, and Vision. Scientific American Book*. New York: W.H. Freeman & Co.

Hubel, D. H., & Wiesel, T. N. (1962). Receptive field, bincoular interaction, and functional architecture in the cat's visual cortex. *Journal of Physiology*, *160*, 106–154.

Hubel, D. H., & Wiesel, T. N. (1967). Cortical and callosal connections concerned with the vertical meridian of visual fields in the cat. *Journal of Neurophysiology*, *30*, 1561–1573.

Hubel, D. H., & Wiesel, T. N. (1974). Uniformity of monkey striate cortex: a parallel relationship between field size, scatter, and magnification factor. *Journal of Comparative Neurology*, *158*, 295–306.

Hubel, D. H., & Wiesel, T. N. (1977). Functional architecture of macaque monkey visual cortex. *Proceedings of the Royal Society London*, *Series B*, *198*, 1–59.

Hudson, T., Li, W., & Matin, L. (1997). The perception of visual pitch does not determine visually perceived eye level. *Investigative Ophthalmology and Visual Science*, *38/4*, S1008.

Hudson, T., Li, W., & Matin, L. (2000). Independent mechanisms produce visually perceived eye level (VPEL) and perceived visual pitch. *Vision Research*, *40*, 2605–2619.

Johnston, D., & Wu, S. M. (1995). *Foundations of cellular neurophysiology*. Cambridge, MA: MIT Press.

Johnston, D., Magee, J. C., Colbert, C. M., & Christie, B. R. (1996). Active properties of neuroanl dendrites. *Annual Review of Neuoscience*, *19*, 165–186.

Lackner, J. R. (1978). Some mechanisms underlying sensory and postural stability in man. Ch. 26. In R. Held, H. W. Leibowitz, & H. Teuber, *Handbook of Sensory Physiology*, vol. VIII (pp. 805–846). New York: Springer-Verlag.

Lackner, J. R., & Graybiel, A. (1978). Some influences of touch and pressure cues on human spatial orientation. *Aviation*, *Space and Environmental Medicine*, *49*, 798–804.

LeVay, S., & Sherk, H. (1981a). The visual claustrum of the cat. I. Structure and connections. *Journal of Neuroscience*, *1*, 956–980.

LeVay, S., & Sherk, H. (1981b). The visual claustrum of the cat. II. The visual field map. *Journal of Neuroscience*, *1*, 981–992.

Li, W., Dallal, N., & Matin, L. (2001). Influences of visual pitch and visual yaw on visually perceived eye level (VPEL) and straight ahead (VPSA) for erect and rolled-to-horizontal observers. *Vision Research*, *41*, 2871–2892.

Li, W., & Matin, L. (1990a). Saccadic suppression of displacement. Influence of postsaccadic exposure duration and of saccadic stimulus elimination. *Vision Research*, *30*, 445–455.

Li, W., & Matin, L. (1990b). The influence of saccade length on the saccadic suppression of displacement detection. *Perception and Psychophysics*, *48*, 453–458.

Li, W., & Matin, L. (1990c). Perceived eye level: sensitivity to pitch of a vertical two-line stimulus grows with eccentricity but is biased by elevation. *Investigative Ophthalmology and Visual Science*, *31*(4), 84.

Li, W., & Matin, L. (1991a). Spatial summation of influences on visually perceived eye level from a single variably-pitched 1-line stimulus. *Investigative Ophthalmology & Visual Science*, *32*, 1272.

Li, W., & Matin, L. (1991b). The influence of visual pitch on visually perceived eye level is spatiotopic. *Bulletin of the Psychonomic Society*, *29*(6), 488.

Li, W., & Matin, L. (1992). Rotation in depth of linear arrays of points systematically influences egocentric localization. *Bulletin of the Psychonomic Society*, *30*, 439.

Li, W., & Matin, L. (1993). Eye and head position, visual pitch and perceived eye level. *Investigative Ophthalmology and Visual Science*, *34*, 1311.

Li, W., & Matin, L. (1995a). Differences in influence between pitched-from-vertical and slanted-from-frontal horizontal lines on egocentric localization. *Perception and Psychophysics*, *57*, 71–83.

Li, W., & Matin, L. (1995b). Influences on visually perceived eye level by tilted lines in a frontoparallel plane. *Investigative Ophthalmology and Visual Science*, *36*, S669.

Li, W., & Matin, L. (1996). Visually perceived eye level is influenced identically by lines from erect and pitched planes. *Perception*, *25*, 831–852.

Li, W., & Matin, L. (1997a). Saccadic suppression of displacement: separate influences of saccade size and of retinal eccentricity. *Vision Research*, *37*, 1779–1797.

Li, W., & Matin, L. (1997b). Spatial summation of influences on visually perceived eye level by three differently-pitched lines. *Investigative Ophthalmology and Visual Science*, *38*, S1008.

Li, W., & Matin, L. (1998). Change in visually perceived eye level without change in perceived pitch. *Perception*, *27*, 553–572.

Li, W., & Matin, L. (1999). Two dimensional manual mapping of visual space change induced by pitched-from-vertical line. *Investigative Ophthalmology and Visual Science*, *40*, S800.

Li, W., & Matin, L. (2001a). Influence of lines with different eccentricities on visually perceived eye level. *Investigative Ophthalmology & Visual Science*, *42/4*, 5404.

Li, W. & Matin L. (2001b). Distance-contingent accuracy of pointing to a perceptually mislocated target. *Proceedings of the third International Conference on Cognitive Science*, 251.

Li, W., Hudson, T., & Matin, L. (2000). Perceiving surface pitch is not involved in producing the influence on visually perceived eye level (VPEL) from lines on that surface. *Investigative Ophthalmology & Visual Science*, *(41)*, *4*, S724.

Lund, J. S., & Boothe, R. G. (1975). Interlaminer connections and pyramidal neuron organization in the visual cortex, area 17, of the macaque monkey. *Journal of Comparative Neurology*, *159*, 305–334.

Lund, J. S., Lund, R. D., Hendrickson, A. E., Bunt, A. H., & Fuchs, A. F. (1975). Origin of efferent pathways from the primary visual cortex, area 17, of the macaquae monkey as shown by retrograde transport of horseradish peroxidase. *Journal of Comparative Neurology*, *164*, 287–304.

Mainen, Z. F., & Sejnowski, T. J. (1998). Modeling active dendritic processes in pyramidal neurons, Ch. 5. In C. Koch, & I. Segev, *Methods in neuronal modeling* (2nd ed., pp. 171–210). Cambridge, MA: MIT Press.

Matin, L. (1968). Critical duration, the differential luminance threshold, critical flicker frequency, and visual adaptation: a theoretical treatment. *Journal of the Optical Society of America*, *58*, 404–415.

Matin, L. (1972). Eye movements and perceived visual direction, Ch. 13. In D. Jameson, & L. Hurvich, *Handbook of sensory physiology*, *Pt*. 4, vol. VII (pp. 331–380). Heidelberg: Springer-Verlag.

Matin, L. (1982). Visual localization and eye movements. In A. Wertheim, W. A. Wagenaar, & H. Leibowitz, *Tutorials on motion perception* (pp. 101–156). New York: Plenum Press.

Matin, L. (1986). Visual localization and eye movements. In K. Boff, L. Kaufman, & J. Thomas, *Handbook of perception and human performance*, *Ch*. 20, vol. I (pp. 20-1–20-45). New York: Wiley.

Matin, L., & Fox, C. R. (1986). Perceived eye level: elevation jointly determined by visual field pitch, EEPI, and gravity. *Investigative Ophthalmology and Visual Science (Suppl.)*, *27*, 333.

Matin, L., & Fox, C. R. (1989). Visually perceived eye level and perceived elevation of objects: linearly additive influences from visual field pitch and from gravity. *Vision Research*, *29*, 315–324.

Matin, L., & Li, W. (1989). Linear summation of visual influences on perceived eye level. *Journal of the Optical Society of America*, *Technical Digest Series*, *Annual Meeting*, *18*, 161.

Matin, L., & Fox, C. R. (1990). Erratum. Visually perceived eye level and perceived elevation of objects: linearly additive influences from visual field pitch and from gravity. *Vision Research*, *30*, 1.

Matin, L., & Li, W. (1991). Separate mechanisms for perceived eye level and perceived vertical: dissection by pitch and roll of a two-line stimulus. *Investigative Ophthalmology and Visual Science (Suppl.)*, *32*, 900.

Matin, L., & Li, W. (1992a). Visually perceived eye level: changes induced by a pitched-from-vertical two-line visual field. *Journal of Experimental Psychology: Human Perception and Performance*, *18*, 257–289.

Matin, L., & Li, W. (1992b). Mislocalizations of visual elevation and visual vertical induced by visual pitch: the Great Circle Model. *Annals of the New York Academy of Sciences USA*, *656*, 242–265.

Matin, L., & Li, W. (1994a). The influence of the orientation of a stationary single line in darkness on the visual perception of eye level. *Vision Research*, *34*, 311–330.

Matin, L., & Li, W. (1994b). Spatial summation among parallel lines across wide separation (50°): spatial localization and the Great Circle Model. *Vision Research*, *34*, 2577–2598.

Matin, L., & Li, W. (1994c). Mirror symmetry and parallelism: two opposite rules for the identity transform in space perception and their unified treatment by the Great Circle Model. *Spatial Vision*, *8*, 469–489.

Matin, L., & Li, W. (1995a). Multimodal basis for egocentric spatial localization and orientation. *Journal of Vestibular Research*, *5*, 499–518.

Matin, L., & Li, W. (1995b). Light and dark adaptation of visually perceived eye level controlled by visual pitch. *Perception and Psychophysics*, *57*, 84–104.

Matin, L., & Li, W. (1997a). PDP model for the influence of line orientation on visually perceived eye level. *Investigative Ophthalmology and Visual Science*, *38/4*, S1008.

Matin, L. & Li, W. (1997b). Spatial vision: from the stimulus through the single nerve membrane to perception. *38th Annual meeting of the psychonomic society*, p. 35.

Matin, L., & Li, W. (1997c). Summation and averaging of visual influences on VPEL modeled by postsynaptic conductance change in orientation-selective system. *Abstract of Society for Neuroscience*, *23*, 175.

Matin, L., & Li, W. (1998). Combining orientations for the perception of space. *Investigative Ophthalmology and Visual Science*, *39/4*, S669.

Matin, L., & Li, W. (1999a). Averaging and summation of influences on visually perceived eye level between two long lines differing in pitch or roll-tilt. *Vision Research*, *39*, 307–329.

Matin, L., & Li, W. (1999b). Two roll-tilted inducing lines average their influences on the orientation of visually perceived vertical (VPV). *40th Annual Meeting of the Psychonomic Society*, *4*, 37.

Matin, L., & Li, W. (2000). Linear combination of signals from two lines of the same or different orientations. *Vision Research*, *40*, 517–527.

Matin, L., & Li, W. (2001). Decomposition of the frame's influence. II. Short lines. *Investigative Ophthalmology & Visual Science*, *(42)*, *4*, S121.

Matin, L., Li, W., Hudson, T., & Hirsch, J. (2001). Perceptions of elevation and orientation: From the stimulus basis to the cerebral cortex. *1st Annual Meeting of Vision Sciences Society*, *1*, 56.

Matin, L., Picoult, E., Stevens, J. K., Edwards, M. W. Jr, Young, D., & MacArthur, R. (1982). Oculoparalytic illusion: visual-field dependent mislocalizations by humans partially paralyzed with curare. *Science*, *216*, 198–201.

Matin, L., Stevens, J. K., & Picoult, E. (1983). Perceptual consequences of experimental extraocular muscle paralysis. In A. Hein, & M. Jeannerod, *Spatially oriented behavior*, *Ch.* 14 (pp. 243–262). New York: Springer.

McCourt, M. E., Boyapati, J., & Henry, G. H. (1986). Layering in lamina 6 of cat striate cortex. *Brain Research*, *364*, 181–185.

Nemire, K., & Cohen, M. M. (1993). Visual and somesthetic imfluences on postural orientation in the median plane. *Perception and Psychophysics*, *53*, 106–116.

Poquin, D., Ohlmann, T., & Barraud, P. A. (1998). Isotropic visual field effect on spatial orientation and egocentric localization. *Spatial Vision*, *11*, 261–278.

Post, R. B., & Welch, R. B. (1996). The role of retinal versus perceived size in the effects of pitched displays on visually perceived eye level. *Perception*, *25*, 853–859.

Post, R. B., Welch, R. B., & Clark, V. D. (2000). Why do pitched horizontal lines have such a small effect on visually perceived eye level? *Perception and Psychophysics*, *62*, 726–734.

Raphel, C., & Barraud, P. A. (1994). Perceptual thresholds of radial accelerations as indicated by visually perceived eye level. *Aviation*, *Space and Environmental Medicine*, *65*, 204–208.

Raphel, C., Barraud, P. A., Koessler, C., & Cian, C. (1996). Effects of a visual frame and of low radial accelerations on the visually perceived eye level. *Perception and Psychophysics*, *58*, 906–914.

Robison, E., Li, W., & Matin, L. (1995). Manual matches to the elevation of visually mislocalized targets. *Investigative Ophthalmology and Visual Science*, *36*, S358.

Servos, P., Matin, L., & Goodale, M. (1993). Visually perceived eye level in a visual form agnosic. *Investigative Ophthalmology and Visual Science*, *34*, 1416.

Servos, P., Matin, L., & Goodale, M. A. (1995). Dissociation between two modes of spatial processing by a visual form agnosic. *NeuroReport*, *6*, 1893–1896.

Shepherd, G. M. (1998). *The synaptic organization of the brain* (4th edn). New York: Oxford University Press.

Sherk, H., & LeVay, S. (1981). The visual claustrum of the cat. III. Receptive field properties. *Journal of Neuroscience*, *1*, 993–1002.

Sherk, H., & LeVay, S. (1983). Contribution of the cortico-claustral loop to receptive field properties in area 17 of the cat. *Journal of Neuroscience*, *3*, 2121–2127.

Sherrington, C. (1929). Ferrier lecture. Some functional problems attaching to convergence. *Proceedings of the Royal Society of London*, *Series B*, *105*, 332–362.

Stoper, A. E., & Bautista, A. B. (1991). The effect of pitched environment on apparent height: task dependence. *Bulletin of the Psychonomic Society*, *29*(6), 526.

Stoper, A., & Cohen, M. M. (1989). Effect of structured visual environments on apparent eye level. *Perception and Psychophysics*, *46*, 469–475.

Ts'o, D. Y., Gilbert, C. D., & Wiesel, T. N. (1986). Relationships between horizontal interactions and functional architecture in cat striate cortex as revealed by cross-correlation analysis. *Journal of Neuroscience*, *6*, 1160–1170.

Welch, R. B., & Post, R. B. (1996). Accuracy and adaptation of reaching and pointing in pitched visual environments. *Perception and Psychophysics*, *58*, 383–389.

Welch, R. B., Post, R. B., Lum, W., Kang, M., Napoli, C., & Cohen, M. M. (1998). Adapting to a pitch room. *39th Annual Meeting of the Psychonomic Society*, *3*, 14.

Witkin, H. A. (1949). Perception of body position and of the position of the visual field. *Psychology Monograph*, *63*(7), 1–46.

Witkin, H. A., & Asch, S. E. (1948). Studies in space perception: IV. Further experiments on perception of the upright with displaced visual fields. *Journal of Experimental Psychology*, *38*, 762–782.

Yuste, R., & Tank, D. W. (1996). Dendritic integration in mammalian neurons: a century after Cajal. *Neuron*, *16*, 701–716.

Zeki, S. (1986). The anatomy and physiology of area V6 of macaque monkey visual cortex. *Journal of Physiology*, *381*, 62p.

Zeki, S. (1993). *A Vision of the Brain*. Oxford: Blackwell Scientific Publications.